

RESEARCH ARTICLE

Phytochrome-interacting factors orchestrate hypocotyl adventitious root initiation in *Arabidopsis*

Qian-Qian Li^{1,2}, Zhan Zhang¹, Chao-Xing Zhang^{1,3}, Ya-Ling Wang¹, Chu-Bin Liu^{1,2}, Jia-Chen Wu^{1,2}, Mei-Ling Han¹, Qiu-Xia Wang⁴ and Dai-Yin Chao^{1,*}

ABSTRACT

Adventitious roots (ARs) are an important type of plant root and display high phenotypic plasticity in response to different environmental stimuli. It is known that photoreceptors inhibit darkness-induced hypocotyl adventitious root (HAR) formation by directly stabilizing Aux/IAA proteins. In this study, we further report that phytochrome-interacting factors (PIFs) plays a central role in HAR initiation by simultaneously inducing the expression of genes involved in auxin biosynthesis, auxin transport and the transcriptional control of root primordium initiation. We found that, on the basis of their activity downstream of phytochrome, PIFs are required for darkness-induced HAR formation. Specifically, PIFs directly bind to the promoters of some genes involved in root formation, including auxin biosynthesis genes *YUCCA2* (*YUC2*) and *YUC6*, the auxin influx carrier genes *AUX1* and *LAX3*, and the transcription factors *WOX5/7* and *LBD16/29*, to activate their expression. These findings reveal a previously uncharacterized transcriptional regulatory network underlying HAR formation.

KEY WORDS: Auxin, Darkness, Adventitious root, PHYTOCHROME-INTERACTING FACTOR (PIF), *Arabidopsis*

INTRODUCTION

Adventitious roots (ARs) are important components of root system architecture. Multiple endogenous and environmental factors regulate adventitious rooting (Bellini et al., 2014). Previous studies have shown that auxin accumulation is a crucial step in triggering the initiation of root primordia and is mainly regulated by auxin biosynthesis and transport (Verstraeten et al., 2014; Xu, 2018). In *Arabidopsis thaliana*, 11 *YUCCA* (*YUC*) gene family members encoding flavin monooxygenases catalyze the rate-limiting step in auxin biosynthesis and the conversion of indolepropionic acid (IPA) to indoleacetic acid (IAA) (Zhao et al., 2001; Cheng et al., 2006). *YUC*-mediated endogenous auxin biosynthesis is required for biological processes; e.g. *YUC1* and *YUC4* are induced by wounding, and the expression of *YUC5*, *YUC8* and *YUC9* increases marginally in response to darkness, while *YUC2* and *YUC6* primarily contribute to maintenance of basal

auxin levels (Chen et al., 2016). Previous studies have shown that *YUC6* is expressed in hypocotyl adventitious root (HAR) primordial (Della Rovere et al., 2013; Velocchia et al., 2016); however, the roles of *YUC* genes in HAR formation remain unknown.


Auxin transport also plays a crucial role in adventitious rooting (Lakehal and Bellini, 2019). PIN-FORMED (PIN) and P-glycoprotein (ABCB/PGP) transport proteins are major auxin efflux carriers, while AUXIN1/LIKE-AUX1 (AUX/LAX) proteins are major auxin influx carriers (Swarup and Peret, 2012; Grones and Friml, 2015). PIN1 and PIN6 have been reported to play opposite roles in HAR formation (Della Rovere et al., 2013; Simon et al., 2016). Moreover, *PIN1* and *ABCB19* are involved in adventitious rooting from plants whose roots have been removed; in particular, the transcription of *ABCB19* is rapidly induced upon root excision, which increases auxin transport and accumulation in the basal region of the hypocotyl, and ultimately drives the formation of ARs (Sukumar et al., 2013). In addition, some studies have reported that the coordinated activity of PIN1, AUX1 and LAX3 causes auxin to accumulate and maintains auxin at maximum levels during HAR formation (Della Rovere et al., 2013, 2015; Velocchia et al., 2016). However, how these factors are regulated in HAR formation remains unclear.

Light is an important environmental factor that suppresses HAR formation; specifically, photoreceptors interact with and stabilize Aux/IAA14 proteins to inhibit the HAR-positive regulators AUXIN RESPONSE FACTORS (ARF) 7/ARF19, LATERAL ORGAN BOUNDARIES DOMAIN (LBD) 16/LBD29, and WUSCHEL-RELATED HOMEODOMAIN (WOX) 5/WOX7 (Li et al., 2021). However, whether other light signaling components are also involved in HAR initiation is unknown. Phytochrome-interacting factors (PIFs) are basic helix-loop-helix (bHLH) transcription factors (TFs) that accumulate in the dark to promote skotomorphogenesis (Leivar et al., 2008; Zhang et al., 2013). Several studies have reported that PIFs regulate *YUC5*, *YUC8* and *YUC9* expression to increase auxin biosynthesis during the shade-avoidance response (Hornitschek et al., 2012; Li et al., 2012; Sun et al., 2012; Di et al., 2016; Pucciariello et al., 2018). However, whether and how PIFs regulate HAR formation is still unknown.

In this study, we reported that PIFs are central factors involved in darkness-induced HAR development. We found that PIFs improved HAR formation by directly activating *YUC2* and *YUC6*, but not *YUC5*, *YUC8* or *YUC9*. In addition, PIFs mediate the darkness-induced expression of auxin influx carrier-related genes and TF-encoding genes involved in root priming in the hypocotyl to initiate HAR. These findings demonstrate that PIFs regulate HAR formation in darkness by coordinating auxin biosynthesis, auxin transport and TFs involved in root priming. Additionally, these findings reveal a new regulatory mechanism controlling HAR formation, therefore improving our understanding of how darkness induces HAR initiation in *Arabidopsis*.

¹National Key Laboratory of Plant Molecular Genetics, Chinese Academy of Sciences Center for Excellence in Molecular Plant Sciences, Institute of Plant Physiology and Ecology, Chinese Academy of Sciences, Shanghai 200032, China. ²University of Chinese Academy of Sciences, Beijing 100049, China. ³School of Life Science, Henan University, Kaifeng 457000, China. ⁴Institute of Plant Protection, Chinese Academy of Agricultural Sciences, Beijing, 100193, China.

*Author for correspondence (dychao@cemps.ac.cn)

 Z.Z., 0000-0002-8735-2302; C.-X.Z., 0000-0003-2832-4800

Handling Editor: Ykä Helariutta
Received 13 January 2022; Accepted 19 April 2022

RESULTS

PIFs promote the initiation of HARs and wound-induced ARs

Darkness is necessary for HAR formation because photoreceptors inhibit this process by directly interacting with and stabilizing IAA14 proteins (Li et al., 2021). PIF proteins accumulate in the dark and promote skotomorphogenesis in etiolated seedlings (Castillon et al., 2007). However, to address whether PIFs are also involved in the regulation of HAR formation, we grew various *Arabidopsis pif* mutants and wild-type Columbia (Col-0) plants on half-strength Murashige and Skoog (1/2 MS) media for 14 days in the dark. We evaluated the HARs of these plants and found that the HAR formation in the *pif* mutants was defective. Among the single mutants, *pif1-1* and *pif3-7* developed fewer HARs than did the wild-type Col-0 plants, while *pif5-3* developed slightly more HARs than the wild type (Fig. 1A,B). These results indicated that PIF1 and PIF3 contribute to HAR formation, but there might be some compensatory mechanism at play in the *pif5-3* mutants. Quantitative reverse transcription-polymerase chain reaction (qRT-PCR) confirmed that the expression of *PIF1*, *PIF3* and *PIF4* was upregulated in the *pif5-3* mutants (Fig. S1). Furthermore, *pif* double and triple mutants developed significantly fewer HARs than the corresponding single mutants did, and the *pif1 pif3 pif4* (*pif134*) triple mutant developed the fewest HARs among the triple mutants (Fig. 1C-F). In addition, the *pif1 pif3 pif4 pif5* quadruple mutant (*pifq*) did not develop any HARs. Taken together, these data indicate that PIFs are positive regulators and act redundantly in HAR formation.

To confirm this conclusion, we overexpressed Flag-tagged PIFs in Col-0 plants. Overexpression of *PIF1-Flag* significantly increased HAR numbers in both darkness and red light (Fig. 2A,B and Fig. S2A,B). Moreover, overexpression of *PIF3-Flag*, *PIF4-Flag* and *PIF5-Flag* also promoted HAR formation in

red light but not in the dark (Fig. 2A,B and Fig. S2C-H). In contrast, overexpression of *PIF4-Flag* and *PIF5-Flag* suppressed HAR formation in the dark (Fig. 2A,B). We performed immunoblot assays to detect the levels of PIF-Flag proteins in all four *PIF-Flag* overexpression lines under darkness and red light, and found that *PIF4-Flag* and *PIF5-Flag* overexpression lines produced PIF4-Flag and PIF5-Flag levels that were notably higher than the PIF1-Flag and PIF3-Flag levels in *PIF1-Flag* and *PIF3-Flag* overexpression lines, respectively (Fig. 2C,D). Interestingly, we noticed that ~80% of the hypocotyls of *PIF4-Flag* and *PIF5-Flag* overexpression lines were abnormal (Fig. 2E) and hardly produce HARs under darkness. Moreover, Trypan Blue staining showed that cell death occurred in the stele of the hypocotyls of both the *PIF4-Flag* and *PIF5-Flag* plants (Fig. 2F). Such hypocotyl defects might be a result of abnormal xylem differentiation, given that auxin promotes xylem differentiation (Ursache et al., 2014; Smetana et al., 2019) and PIF4 and PIF5 activate expression of auxin synthesis genes (Li et al., 2012; Sun et al., 2012).

To further investigate the roles of PIFs in AR formation, we further evaluated adventitious rooting of leaf explants of the wild type and *pifq* mutant. Leaf explants of Col-0 and *pifq* were cultured on B5 media for 12 days under darkness. Rooting was significantly reduced in the *pifq* mutant, and the mutant phenotype could be rescued by supplementation with IAA (Fig. S3). Taken together, these results suggest that PIFs also can promote adventitious rooting in leaf explants by affecting auxin levels in the leaves.

PIFs regulate *YUC2* and *YUC6* to control HAR formation

Given that PIFs have been reported to directly regulate the expression of some YUC genes (*YUC5*, *YUC8* and *YUC9*) to promote hypocotyl elongation (Hornitschek et al., 2012; Li et al., 2012;

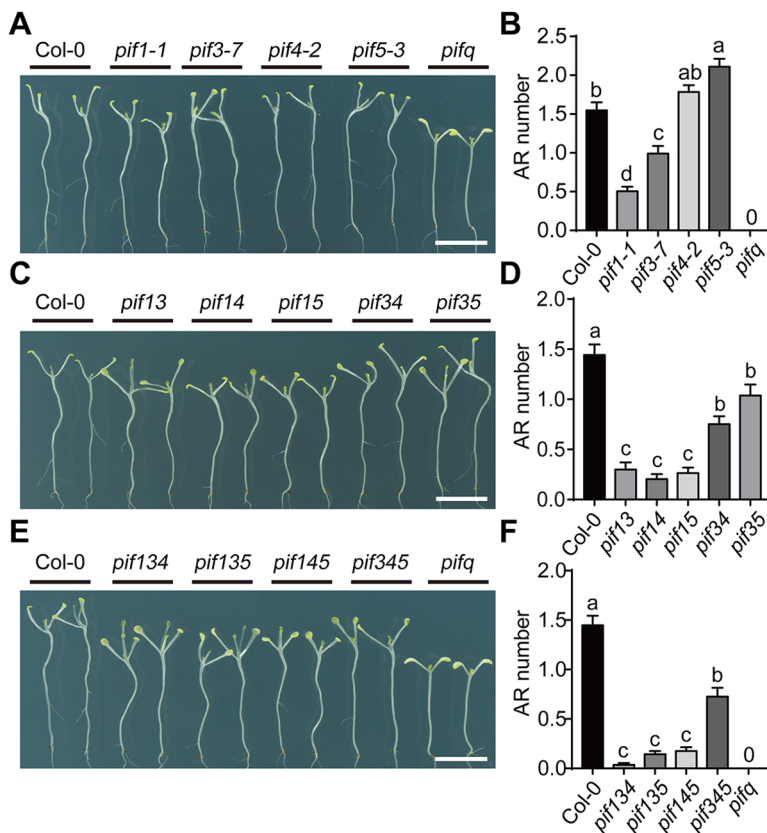


Fig. 1. Initiation of HARs is impaired in the *pif* mutants.

(A) Representative images of 14-day-old Col-0, *pif1-1*, *pif3-7*, *pif4-2*, *pif5-3* and *pifq* seedlings grown in the dark. (B) Quantification of the number of HARs of the plants in A. (C) Representative images of 14-day-old Col-0, *pif1 pif3* (*pif13*), *pif1 pif4* (*pif14*), *pif1 pif5* (*pif15*), *pif3 pif4* (*pif34*) and *pif3 pif5* (*pif35*) seedlings grown in the dark. (D) Quantification of the number of HARs of the plants in C. (E) Representative images of 14-day-old Col-0, *pif1 pif3 pif4* (*pif134*), *pif1 pif3 pif5* (*pif135*), *pif1 pif4 pif5* (*pif145*), *pif3 pif4 pif5* (*pif345*) and *pifq* seedlings grown in the dark. (F) Quantification of the number of HARs of the plants in E. The data in B, D and F are from three independent biological replicates, with each replicate including 30 seedlings. Data are mean ± s.e.m. The different letters above the bars indicate significant differences according to one-way ANOVA and Kruskal-Wallis non-parametric test with post-hoc analysis using Dunn's multiple comparisons test ($P < 0.05$). The 0 above *pifq* indicates that *pifq* developed no HARs. Scale bars: 1 cm.

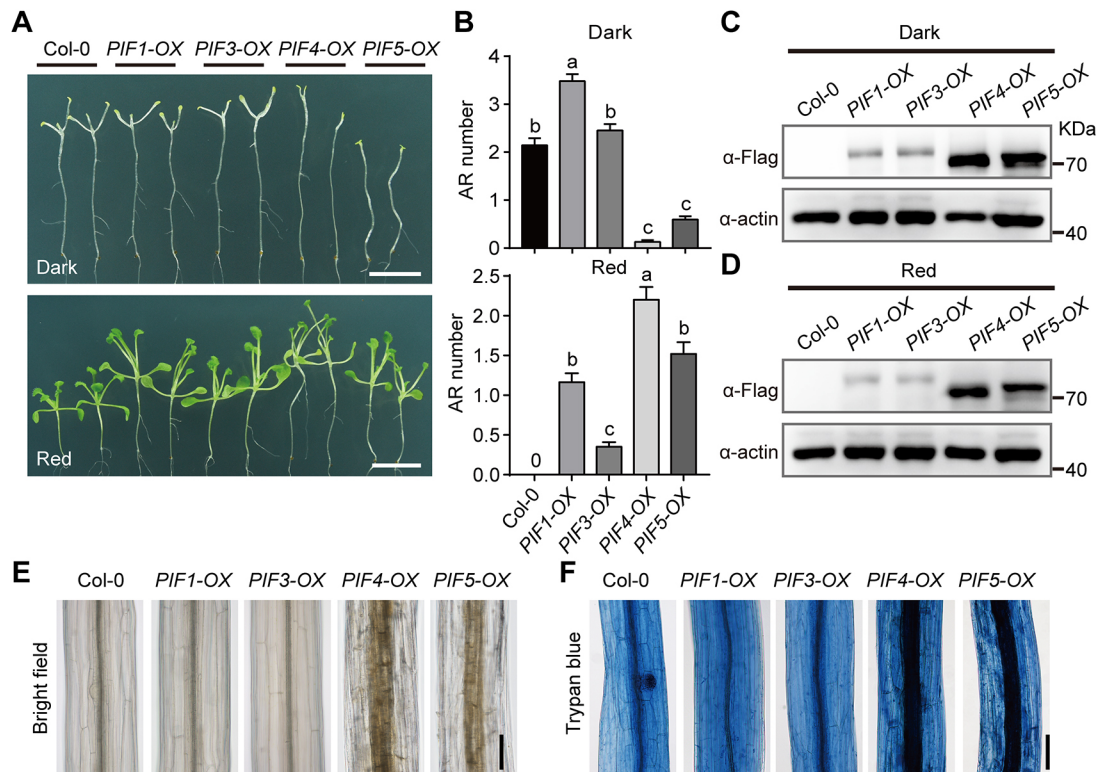


Fig. 2. Overexpression of PIFs promotes HAR formation. (A) Representative images of 14-day-old seedlings of Col-0 and PIF overexpression (*PIFs-OX*) lines grown in darkness or in red light. Scale bars: 1 cm. (B) Quantification of HAR numbers of the plants in A. The data are from three independent biological replicates, with each replicate including 30 seedlings. Data are mean \pm s.e.m. The different letters indicate significant differences according to one-way ANOVA and Kruskal–Wallis non-parametric test with post-hoc analysis using Dunn’s multiple comparisons test ($P < 0.05$). The 0 above Col-0 indicates that Col-0 developed no HARs. (C,D) Immunoblots showing PIF protein levels in 5-day-old Col-0 and PIF overexpression lines grown in darkness or red light. (E,F) Microscopy images of the hypocotyls of Col-0 and PIF-overexpressing lines grown in darkness for 14 days with or without Trypan Blue staining. Scale bars: 100 μ m.

Sun et al., 2012), we were interested in whether PIFs control HAR formation through regulation of these YUC genes. To address this question, we examined HAR formation in *yuc* mutants. Surprisingly, the *yuc589* (*yuc5 yuc8 yuc9*) triple mutant and *yuc14* (*yuc1 yuc4*) double mutant developed HARs similar to those of the wild type (Fig. 3A,B), suggesting that *YUC1*, *YUC4*, *YUC5*, *YUC8* and *YUC9* are not necessary for HAR development. In contrast, compared with the wild type, the *yuc26* (*yuc2 yuc6*) double mutant developed significantly fewer HARs (Fig. 3A–D). Compared with the wild type, the *yuc2* and *yuc6* single mutants also developed significantly fewer HARs, while *yuc26* developed fewer HARs than did *yuc2* or *yuc6* (Fig. 3C,D). These results indicate that *YUC2* and *YUC6* act redundantly in HAR formation.

Supporting the conclusion that YUC genes are required for HAR formation, we found that Col-0 seedlings were not able to develop HARs by yucasin treatment (Fig. S4A,B). Furthermore, when we introduced the *DR5:: β -glucuronidase* (*GUS*) expression construct into *pifq* by crossing with a *DR5::GUS* transgenic line in the Col-0 background, we found that GUS signals were obviously weaker in *pifq* than in Col-0 (Fig. S5), indicating that PIFs are required for auxin homostasis. Together, these data indicated that PIFs might regulate HARs through the regulation of *YUC2* and *YUC6*. To confirm this, we examined the expression of *YUC2* and *YUC6* in the hypocotyls of Col-0 and *pifq* mutants by using qRT-PCR. We found that the expression of *YUC2* and *YUC6* significantly decreased in the *pifq* mutant (Fig. 3E). In addition, we also generated promoter-*GUS* reporter lines for the *YUC2* and *YUC6* genes in the wild-type and *pifq* background. GUS staining

assays showed that the expression of *YUC2* and *YUC6* significantly decreased in the hypocotyls of the *pifq* mutant (Fig. S6). Interestingly, *YUC2* and *YUC6* were also induced in the hypocotyls by darkness (Fig. S7A,B), which is consistent with the accumulation of PIFs in the darkness-treated hypocotyls (Lorrain et al., 2008; Shen et al., 2008; Soy et al., 2012; Ni et al., 2013).

To test whether PIFs directly regulate the expression of *YUC2* and *YUC6*, we performed a dual-luciferase (dual-LUC) assay in *Arabidopsis* protoplasts. We found that the expression of *pYUC2-LUC* and *pYUC6-LUC* increased when PIFs were co-expressed (Fig. 3F,G). To further test whether PIFs could directly bind the promoters of *YUC2* and *YUC6*, we generated recombinant His-PIF1 proteins and performed a gel electrophoretic mobility shift assay (EMSA) with the *YUC2* or *YUC6* promoter fragments containing the E-box motif or PBE-box motif, respectively. Our data showed that PIF1 could directly bind to the promoter fragments of *YUC2* and *YUC6* (Fig. 4A,D). Furthermore, using *PIF1-Flag* transgenic plants, we performed a chromatin immunoprecipitation (ChIP)-qPCR assay, the result of which confirmed that PIF1 binds to the promoters of *YUC2* and *YUC6* *in vivo* (Fig. 4B,E). We also performed ChIP-qPCR with the *PIF4-Flag* overexpression line and found that the predicted PIF-binding fragments of the *YUC2* and *YUC6* promoters precipitated to a much greater degree in this line than in the *PIF1-Flag* transgenic line (Fig. 4C,F), most likely the result of the high level of PIF4 (Fig. 2C,D). Together, these results demonstrated that PIFs activate the expression of *YUC2* and *YUC6* by directly binding to cis-elements of these two genes.

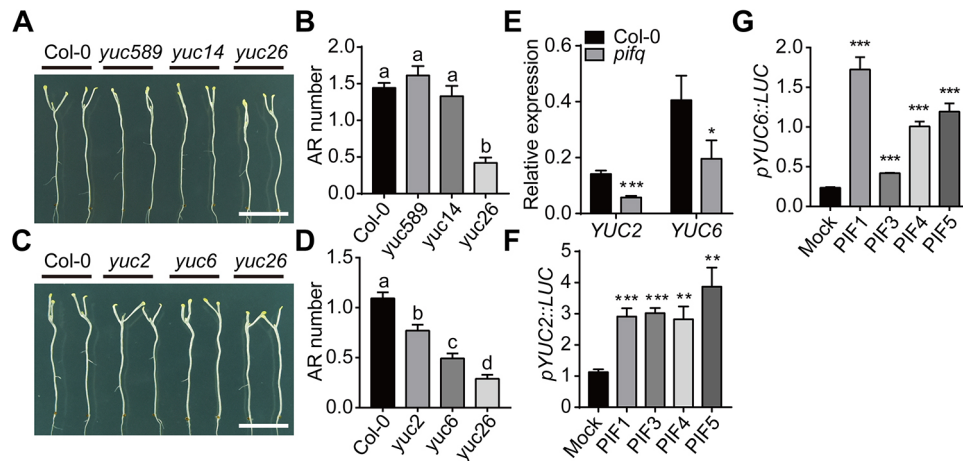


Fig. 3. PIFs promote the expression of *YUC2* and *YUC6* in hypocotyls in darkness. (A) Representative images of 14-day-old Col-0, *yuc589 yuc8 yuc9* (*yuc589*), *yuc1 yuc4* (*yuc14*) and *yuc2 yuc6* (*yuc26*) seedlings grown in the dark. (B) Quantification of the number of HARs of the plants in A. (C) Representative images of 14-day-old Col-0, *yuc2*, *yuc6* and *yuc2 yuc6* (*yuc26*) seedlings grown in the dark. (D) Quantification of the number of HARs of the plants in C. The data in B and D are from three independent biological replicates, with each replicate including 30 seedlings. Data are mean \pm s.e.m. The different letters indicate significant differences according to one-way ANOVA and Kruskal–Wallis non-parametric test with post-hoc analysis using Dunn’s multiple comparisons test ($P<0.05$). Scale bars: 1 cm. (E) qRT-PCR results of the expression of *YUC2* and *YUC6* in hypocotyls of plants grown in darkness for 4 days. Data are derived from three biological replicates. Data are mean \pm s.d. The asterisks represent significant differences compared with the wild type according to an unpaired two-tailed Student’s *t*-test (* $P<0.05$; *** $P<0.001$). (F,G) Dual-LUC assays of *pYUC2::LUC* and *pYUC6::LUC* expression. *Arabidopsis* mesophyll protoplasts were transfected with *pYUC2::LUC* (F) and *pYUC6::LUC* (G) constructs expressing PIF1, PIF3, PIF4 and PIF5. The LUC activity was normalized to the REN activity. Data are derived from three biological replicates. Data are mean \pm s.d. The asterisks represent significant differences compared with the empty vector (Mock) according to an unpaired two-tailed Student’s *t*-test (** $P<0.01$; *** $P<0.001$).

Exogenous application of auxin was not able to rescue the HAR phenotype of *pifq*

To address whether the defect in auxin biosynthesis is the only reason for the inability of *pifq* mutants to develop HARs, we applied IAA to Col-0 plants and to *yuc6*, *yuc26* and *pifq* mutants. Surprisingly, we found that IAA could promote HAR formation in Col-0, *yuc6* and *yuc26* mutants, but not in the *pifq* mutant

(Fig. S8A), indicating that auxin biosynthesis is not the only cause of the defective HAR formation in *pifq*. High concentration of IAA also could not rescue the defective HAR formation in *pifq* mutants (Fig. S8B,C).

As exogenous auxin could not complement the defective HAR formation in the *pifq* mutant, we were interested in whether increased levels of endogenous auxin could rescue the phenotype of

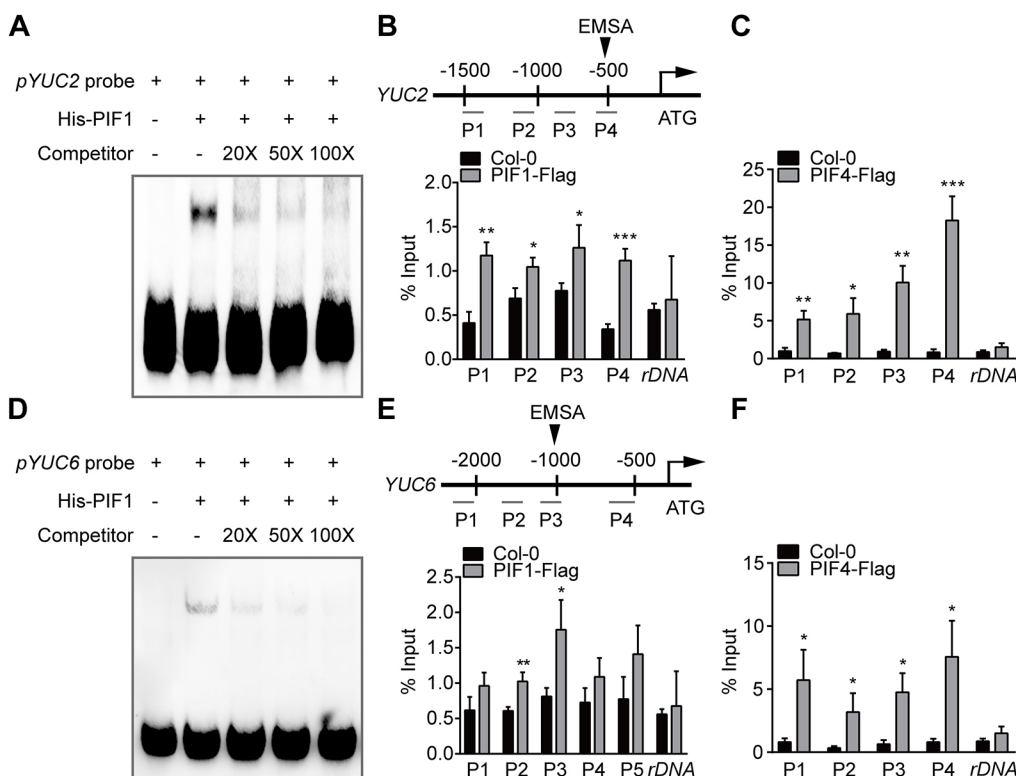


Fig. 4. PIFs directly bind the promoters of *YUC2* and *YUC6* both *in vitro* and *in vivo*. (A,D) EMSA showing that His-PIF1 recombinant proteins bind to biotin-labeled probes of *YUC2* and *YUC6*. (B,C) ChIP assays of *YUC2* in 8-day-old Col-0, *PIF1-Flag* or *PIF4-Flag* seedlings grown under red light for 2 days and then transferred to darkness for 6 days. (E,F) ChIP assays of *YUC6* in 8-day-old Col-0, *PIF1-Flag* or *PIF4-Flag* seedlings grown under red light for 2 days and then transferred to darkness for 6 days. Data in B,C,E and F are derived from three biological replicates. Data are mean \pm s.d. The asterisks represent significant differences compared with the wild type according to an unpaired two-tailed Student’s *t*-test (* $P<0.05$; ** $P<0.01$; *** $P<0.001$).

the *pifq* mutant. To investigate this, we knocked out *SURI* in the *pifq* mutant background via the clustered, regularly interspaced, short palindromic repeat (CRISPR)/CRISPR-associated 9 (Cas9) technology to increase endogenous auxin concentrations (Boerjan et al., 1995). We found that *sur1 pifq* quintuple mutants presented high numbers of ARs, and their phenotype was similar to that of *sur1* (Fig. S8D). Taken together, these results indicated that PIFs might regulate HAR formation by affecting auxin influx.

PIFs promote the expression of *AUX1* and *LAX3* to initiate HARs

Given that endogenous but not exogenous auxin could complement the defective HAR formation in the *pifq* mutant, we hypothesized that PIFs are also required for auxin transport. To test this hypothesis, we examined whether the expression of *AUX1* and *LAX3*, two genes encoding auxin influx carriers, is regulated by PIFs. qRT-PCR showed that the transcript abundances of *AUX1* and *LAX3* were lower in the hypocotyls of *pifq* than in those of the wild type in darkness (Fig. 5E,F). These results suggested that PIFs promote the transcription of *AUX1* and *LAX3* in darkness. Moreover, GUS staining assays showed that the expression of *AUX1* and *LAX3* significantly decreased in the hypocotyl of the *pifq*

mutant (Fig. S9), the results of which were consistent with the qRT-PCR results. Additionally, the *AUX1_{pro}:AUX1-GFP* reporter construct revealed that *AUX1* was high expressed in the stele and the HAR primordia of wild type, but was apparently low in that of *pifq* (Fig. 5G). Similarly, the reduced expression of *LAX3_{pro}:LAX3-GFP* was also observed in the stele tissues in the hypocotyl of *pifq* mutant (Fig. 5H). Furthermore, both *AUX1* and *LAX3* were induced in hypocotyls by darkness (Fig. S7C,D), which is consistent with the role of PIFs in enhancing *AUX1* and *LAX3* expression.

Given that *AUX1* and *LAX3* are regulated by PIFs, we speculated that influx of auxin into the cells is required for HAR initiation. Consistent with this hypothesis, we found that the number of HARs was suppressed by treatment with the auxin influx inhibitor 1-naphthoxyacetic acid (1-NOA) (Fig. S4C,D). In addition, we found that the number of HARs of the *aux1* and *lax3* mutants were decreased compared with those of the wild type, and *aux1* developed fewer HARs than *lax3* did, suggesting that both *AUX1* and *LAX3* play roles in HAR formation, while *AUX1* plays a stronger role. Moreover, compared with the two single mutants, the *aux1 lax3* double mutant developed significantly fewer HARs, indicating that *AUX1* and *LAX3* act redundantly in terms of HAR formation (Fig. 5A,B). In contrast to *aux1* and *lax3*, compared with

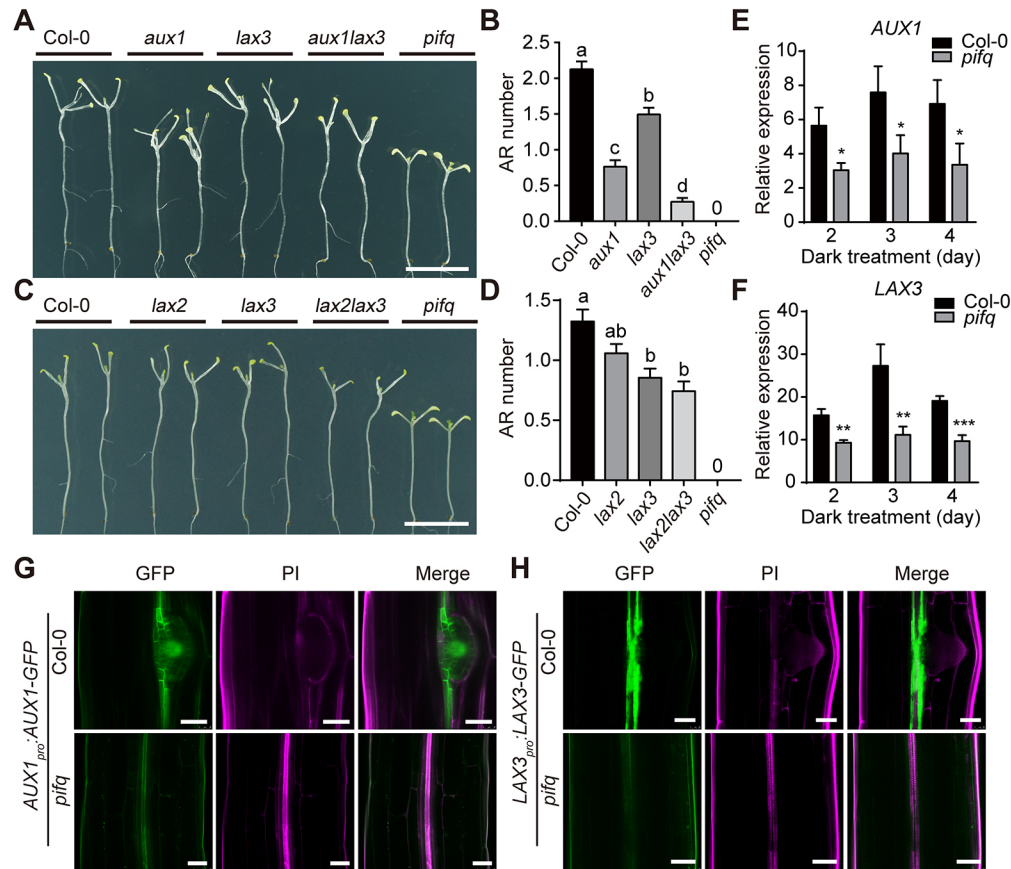


Fig. 5. *AUX1* and *LAX3* contribute to HAR formation and are regulated by PIFs. (A) Representative images of 14-day-old Col-0, *aux1*, *lax3*, *aux1 lax3* and *pifq* seedlings grown in the dark. (B) Quantification of the number of HARs of the plants in A. (C) Representative images of 14-day-old Col-0, *lax2*, *lax3*, *lax2 lax3* and *pifq* seedlings grown in the dark. (D) Quantification of the number of HARs of the plants in C. The data in B and D are from three independent biological replicates, with each replicate including 30 seedlings. Data are mean \pm s.e.m. The different letters indicate significant differences according to one-way ANOVA and Kruskal–Wallis non-parametric test with post-analysis using Dunn’s multiple comparisons test ($P < 0.05$). The 0 above *pifq* indicates that *pifq* developed no HARs. Scale bars: 1 cm. (E, F) qRT-PCR results of *AUX1* (E) and *LAX3* (F) gene expression in the hypocotyls of Col-0 and *pifq* mutants grown in the light for 1 day and then transferred to darkness for 2, 3 and 4 days. Data are derived from three biological replicates. Data are mean \pm s.d. The asterisks represent significant differences compared with the wild type according to an unpaired two-tailed Student’s *t*-test (* $P < 0.05$; ** $P < 0.01$; *** $P < 0.001$). (G, H) Representative confocal microscopy images of 8-day-old hypocotyls with *AUX1_{pro}:AUX1-GFP*, *AUX1_{pro}:AUX1-GFP/pifq* (G), *LAX3_{pro}:LAX3-GFP* or *LAX3_{pro}:LAX3-GFP/pifq* (H) constructs in darkness for 6 days. Cell walls were stained with propidium iodide (PI). Scale bars: 50 μ m.

the wild type, the *lax2* mutant developed similar numbers of HARs, indicating that *LAX2* might not regulate HAR formation (Fig. 5C, D). These results, together with the expression evidence, showed that PIFs promote HAR formation through regulation of *AUX1* and *LAX3*.

PIFs directly bind to the E-box and G-box motifs of the *AUX1* and *LAX3* promoters

To test whether PIFs directly activate *AUX1* and *LAX3* to improve HAR formation, we assessed the promoters of *AUX1* and *LAX3*. We identified several typical PIF-binding sites (G-box, PBE-box and E-box motifs) in these two promoters. Yeast one-hybrid (Y1H) experiments showed that all four PIFs could bind the E-box motif in the promoter of *AUX1* (Fig. 6A,B). In contrast, PIFs could not bind these promoters when the E-box was mutated, suggesting that the binding was specific (Fig. 6A,B). Furthermore, we performed

transient transcription assays in protoplasts to analyze whether PIFs could activate *AUX1* and *LAX3* transcription *in vivo*. Our data showed that co-expression of PIF proteins strongly promoted the activity of LUC reporters driven by the promoters of *AUX1* and *LAX3* (Fig. 6C,D), suggesting that PIFs directly activate the expression of *AUX1* and *LAX3*.

To further confirm this binding, we generated a recombinant His-PIF1 protein and performed EMSAs together with *AUX1* and *LAX3* promoter fragments containing the E-box or G-box. Our data showed that PIF1 could bind to the promoter fragments of *AUX1* and *LAX3* (Fig. 6E,F). Furthermore, we carried out ChIP-qPCR assays with *PIF1-Flag* and *PIF4-Flag* transgenic plants, and the results confirmed that PIF1 and PIF4 bound to the promoters of *AUX1* and *LAX3* *in vivo* (Fig. 6G,H). Together, these results demonstrated that PIF proteins can bind to the promoters of *AUX1* and *LAX3*, and activate their expression.

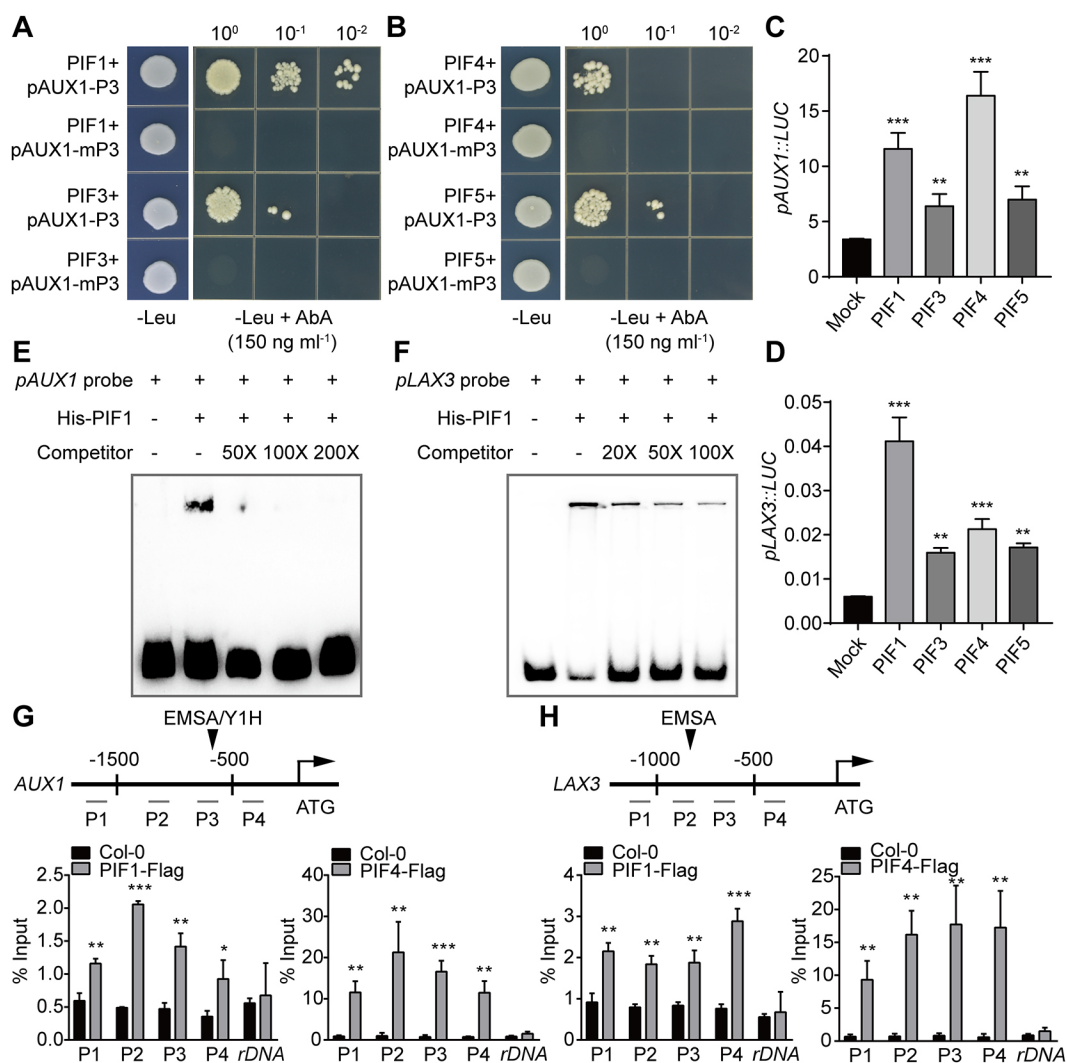


Fig. 6. PIFs directly bind the promoters of *AUX1* and *LAX3* both *in vitro* and *in vivo*. (A,B) Y1H assays showing that PIF1, PIF3, PIF4 and PIF5 can bind to probe 3 (P3) (which contains an E-box motif) but not mutant probe 3 (mP3) (which contains a mutant E-box motif) of the *AUX1* promoter. (C,D) Dual-luciferase assays of *pAUX1::LUC* and *pLAX3::LUC* expression. *Arabidopsis* mesophyll protoplasts were transfected with *pAUX1::LUC* (C) and *pLAX3::LUC* (D), and with constructs expressing PIF1, PIF3, PIF4 and PIF5. The LUC activity was normalized to the REN activity. Data are derived from three biological replicates. Data are mean±s.d. The asterisks represent significant differences compared with the empty vector (Mock) according to an unpaired two-tailed Student's *t*-test (***P*<0.01; ****P*<0.001). (E,F) EMSA showing that His-PIF1 recombinant proteins bind to biotin-labeled probes of *AUX1* (E) and *LAX3* (F). (G,H) ChIP assays of *AUX1* and *LAX3* in 8-day-old Col-0, *PIF1-Flag* or *PIF4-Flag* seedlings grown under red light for 2 days and then transferred to darkness for 6 days. Data are derived from three biological replicates. Data are mean±s.d. The asterisks represent significant differences compared with the wild type according to an unpaired two-tailed Student's *t*-test (**P*<0.05; ***P*<0.01; ****P*<0.001).

PIFs are required for other processes involved in HAR formation in addition to auxin biosynthesis and transport

To further address the role of *AUX1* in *PIF*-mediated HAR formation, we overexpressed *35S-AUX1* in *pifq*. We generated three independent transgenic lines overexpressing *AUX1* (Fig. S10D) and observed that a few *35S-AUX1/pifq* lines were able to develop HARs in the dark (Fig. S10A-C). These data indicated that overexpression of *AUX1* could only partially complement the HAR defect of *pifq*. Interestingly, the application of IAA increased the number of HARs in Col-0 but did not affect the number of HARs in the *AUX1* overexpression lines in the *pifq* background. These observations supported that *AUX1* acts downstream of PIFs in regulating HAR initiation but that PIFs are likely required for other processes involved in HAR formation.

Naphthaleneacetic acid (NAA) is an auxin analog of IAA and is able to enter cells by passive diffusion (Delbarre et al., 1996). We found that NAA was able to induce the development of greater numbers of HARs in Col-0, *aux1*, *lax3* and *aux1 lax3* but not in the *pifq* mutant (Fig. S10E,F). These data further confirm that PIF is also required for processes involved in HAR formation other than auxin biosynthesis and transport.

PIFs do not affect the AUX/IAA14-ARF7/19 module that regulates HAR formation

Given that we have reported that, by stabilizing IAA14 proteins, phytochrome represses the initiation of HARs (Li et al., 2021), we further wondered whether PIFs regulate phytochromes or directly affect auxin signaling components to regulate HAR initiation. To address these questions, we first investigated the genetic relationship between *PHYB* and PIFs. Our data showed that, like the *pifq* quadruple mutant, the *phyB pifq* quintuple mutant did not develop HARs either in darkness or in red light. In contrast, *phyB* was able to develop HARs either in darkness or red light, while Col-0 developed HARs only in the dark (Fig. S11A,B). These data indicate that PIFs are epistatic to *PHYB* in terms of HAR formation.

We further performed immunoblot assays with anti-IAA14 antibodies to determine the IAA14 protein level in the hypocotyls of wild-type, *phyB*, *pifq* and *phyB pifq* mutant seedlings in darkness and red light. The results showed that accumulation of IAA14 protein was hardly detected in any of the seedlings grown in the dark (Fig. S11C), indicating that the inability of *pifq* to develop HARs is not related to steady IAA14 levels. In addition, although *phyB pifq* did not develop any HARs under red light, the abundance of IAA14 protein in this mutant was also reduced (Fig. S11D). These data further confirmed that PIFs regulate HAR formation not through affecting the stability of IAA14.

We also examined whether PIFs interact with AUX/IAA14-ARF7/19 modules. Yeast two-hybrid (Y2H) experiments showed that PIFs did not interact with either IAA14 or ARF19 proteins that lacked an activation domain (Fig. S12). Moreover, the expression of ARF7 and ARF19 was not affected in the hypocotyls of *pifq* compared with the wild type grown in darkness (Fig. S13). Taken together, these data together support the observation that PIFs do not regulate AUX/IAA14-ARF7/19 modules.

PIFs directly activate the expression of *LBD16*, *LBD29*, *WOX5* and *WOX7* to promote HAR initiation

LBD16, *LBD29*, *WOX5* and *WOX7* encode four essential TFs required for the formation of lateral roots (LRs) and HARs (Liu et al., 2014; Hu and Xu, 2016; Sheng et al., 2017; Li et al., 2021). We examined the expression of these four genes and observed that they were induced by darkness (Fig. S7E-H) but were

downregulated in the *pifq* hypocotyls (Fig. 7A-D). Furthermore, *WOX5_{pro}:GUS* and *LBD16_{pro}:LBD16-GUS* reporter lines also showed that expression of *WOX5* and *LBD16* were not detectable in *pifq* mutant (Fig. 7E,F). Similarly, the confocal images showed that *LBD16-GFP* was expressed in HAR primordia and localized in the nuclei, whereas no GFP fluorescence was observed in *pifq* (Fig. 7G). Such downregulation might be caused by defective auxin biosynthesis or transport in the *pifq* mutant, but it is also possible that PIFs could directly regulate *LBD16/29* and/or *WOX5/7*. To test this hypothesis, we tested whether PIFs could bind the promoter of *LBD16*, *LBD29*, *WOX5* and *WOX7*. Y1H assays showed that PIF1 is indeed able to bind to the promoter fragments of *LBD16* and *LBD29* and *WOX5/7* that contain a potential PIF-binding sequence (Fig. 7H-K). We further performed EMSAs, the results of which confirmed that PIF1 is able to directly bind to the promoter sequences of *LBD16*, *LBD29*, *WOX5* and *WOX7* *in vitro* (Fig. 8A-D). Furthermore, ChIP-qPCR assays demonstrated that PIF1 and PIF4 bound to the promoters of *LBD16*, *LBD29*, *WOX5* and *WOX7* *in vivo* (Fig. 8E-H). Together, these data showed that PIFs directly activate the expression of *LBD16*, *LBD29*, *WOX5* and *WOX7*.

DISCUSSION

Multiple components regulating HAR formation have been identified, including Aux/IAAs, ARFs, photoreceptors, Ago1 and other proteins involved in hormone homeostasis (Sorin et al., 2005; Gutierrez et al., 2009, 2012; Lakehal et al., 2019; Lee et al., 2019; Li et al., 2021). These studies indicated that the initiation of HARs involves a complex process and is initiated with the integration of numerous factors and environmental signals. In this study, we identified PIFs as being essential TFs for the initiation of HARs and ARs. Further studies established that PIFs coordinate multiple processes, including auxin biosynthesis, auxin transport and the transcriptional activation of *LBD16*, *LBD29*, *WOX5* and *WOX7* to trigger HAR initiation (Fig. 9). These findings not only revealed essential regulators involved in HAR formation but also revealed a new mechanism underlying darkness-induced HAR formation.

PIFs are essential TFs for HAR formation

Previous studies have reported that PIFs are expressed in the hypocotyl and that PIF proteins are key components in skotomorphogenesis, including hypocotyl elongation (Bae and Choi, 2008; Zhang et al., 2013). Given that darkness is necessary for HAR formation, we thus speculated that PIFs might be involved in HAR formation. As expected, we found that different *pif* mutants showed various defects in adventitious rooting from hypocotyls; *pifq* quadruple mutants were not able to develop any HARs, verifying that PIFs play both redundant and essential roles in HAR formation (Fig. 1). This conclusion was further supported when PIFs were overexpressed, which resulted in significantly more HAR than the wild type under red light. Surprisingly, compared with the wild type, the *PIF4* and *PIF5* overexpression lines developed fewer HARs in darkness, although the *PIF4* overexpression line developed more HARs than the *PIF1* overexpression line in red light (Fig. 2). Further investigation revealed that the relatively low numbers of HARs of the *PIF4*- and *PIF5*-overexpressing lines might be caused by defects of xylem differentiation, as we observed that ~80% of the hypocotyls overexpressing *PIF4* or *PIF5* exhibited abnormal cell death in the stele (Fig. 2). Previous studies have showed that auxin biosynthesis and influx promote xylem differentiation (Ursache et al., 2014; Smetana et al., 2019), which is reversely related to AR formation (Della Rovere et al., 2015).

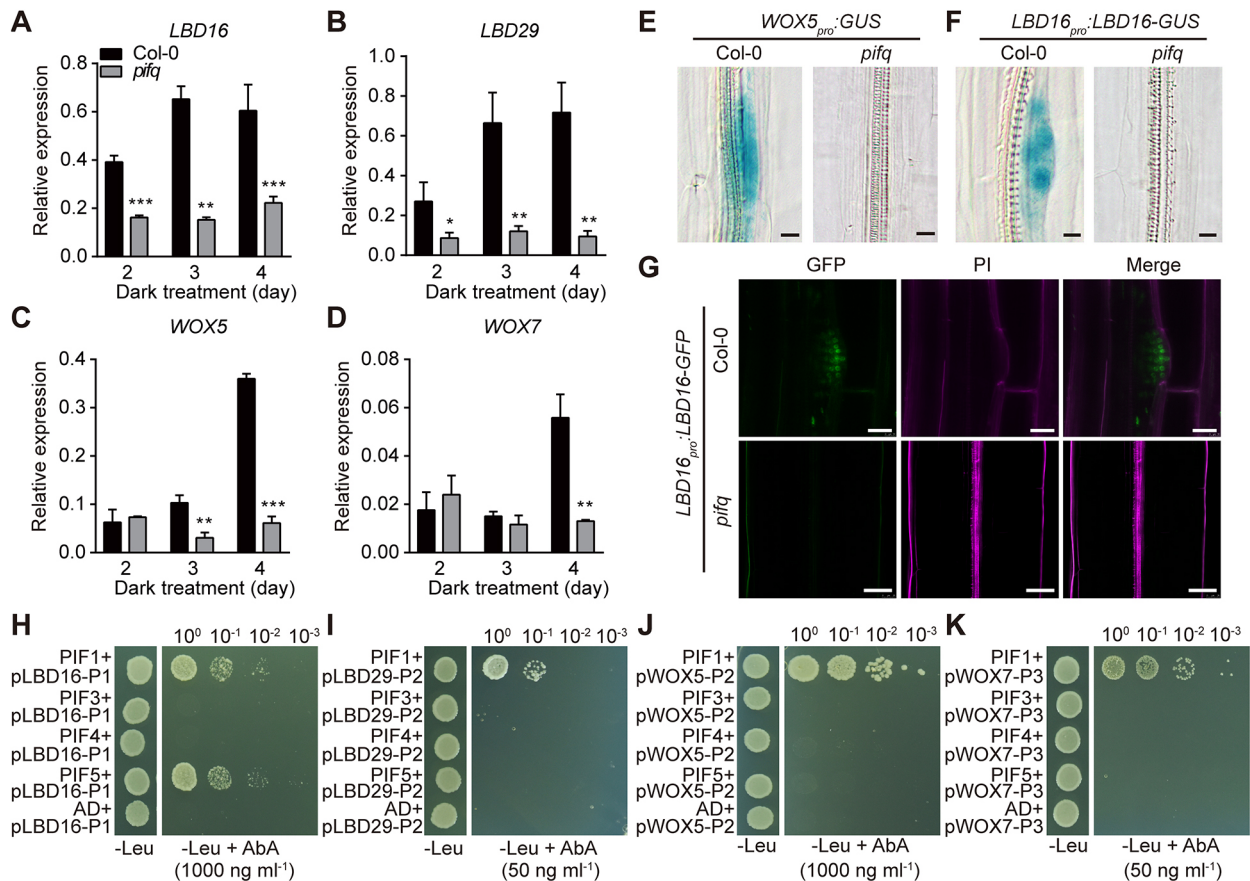


Fig. 7. PIFs activate expression of *LBD16/29* and *WOX5/7*. (A–D) qRT-PCR results of *LBD16*, *LBD29*, *WOX5* and *WOX7* gene expression in the hypocotyls of Col-0 plants and *pifq* mutants grown under white light for 1 day followed by growth under darkness for 2, 3 and 4 days. Data are derived from three biological replicates. Data are mean±s.d. The asterisks represent significant differences compared with the wild type according to an unpaired two-tailed Student's *t*-test (**P*<0.05; ***P*<0.01; ****P*<0.001). (E, F) GUS staining of 6-day-old hypocotyls with *WOX5_{pro}::GUS* (E) and *LBD16_{pro}::LBD16-GUS* (F) in continuous darkness. Scale bars: 20 μm. (G) Confocal microscopy images of 8-day-old *LBD16_{pro}::LBD16-GFP* and *LBD16_{pro}::LBD16-GFP/pifq* hypocotyls in continuous darkness. Cell walls were stained with propidium iodide (PI). Scale bars: 50 μm. (H–K) Y1H assays for the binding of PIF1, PIF3, PIF4 and PIF5 on the PBE-box, G-box or E-box motifs in the *LBD16*, *LBD29*, *WOX5* and *WOX7* promoters.

These data indicate that PIFs might be involved in many more processes than expected, which needs further exploration.

PIFs coordinate HAR formation by simultaneously controlling auxin biosynthesis, auxin transport and essential TFs required for HARs

The initiation of HARs requires the integration of multiple processes, including the perception of environmental signals and the activation of internal regulators. Among them, auxin biosynthesis, transport and signaling are central processes, but it is unknown how these processes are integrated. Previous studies showed that PIFs are able to activate the expression of *YUC5*, *YUC8* and *YUC9* (Hornitschek et al., 2012; Li et al., 2012; Sun et al., 2012). However, our data showed that *YUC5*, *YUC8* and *YUC9* are not required for HAR formation. Instead, we observed that *YUC2* and *YUC6* are essential for HAR formation. Our evidence also indicated that PIFs directly activate the expression of *YUC2* and *YUC6* by binding to the promoters of these genes. A previous study reported that *YUC2* and *YUC6* are involved in adventitious rooting of leaf explants and contribute to basal auxin levels (Chen et al., 2016). Consistently, we found that PIFs are also required for adventitious rooting of leaf explants. Taken together, these data indicated that PIFs could promote auxin synthesis in multiple pathways.

Directional auxin transport in plants is achieved through a combination of auxin transport proteins, including PINFORMED (PIN) efflux carriers, ATP-binding cassette group B (ABC B) auxin transporters and AUX/LAX auxin uptake permeases (Blakeslee et al., 2005; Swarup and Peret, 2012; Grones and Friml, 2015). Previous studies have shown that AUX/LAX auxin uptake permeases contribute to LR and HAR formation (Swarup et al., 2008; Della Rovere et al., 2013, 2015), but how these genes are regulated remains unknown. The identification of PIFs as direct regulators of these genes revealed a new mechanism underlying the regulation of HAR formation.

LBD16/29 and *WOX5/7* encode essential TFs involved in HAR formation, and their expression is controlled by upstream regulators involved in auxin signaling, including IAA14 and ARF7/19. We have reported that PHYB suppresses HAR formation by stabilizing IAA14 proteins. Given that PIFs are PHYB-interacting proteins, it was not unreasonable to speculate that PIFs might also regulate HARs by affecting steady-state IAA14 levels. However, our genetic and molecular evidence demonstrated that PIFs act downstream of PHYB in terms of regulating HAR formation and did not affect steady-state levels of IAA14. Instead, we found that PIFs are able to directly activate the expression of *LBD16/29* and *WOX5/7* to promote HAR formation. These findings indicated that the essential TFs for priming of HAR primordia are not only

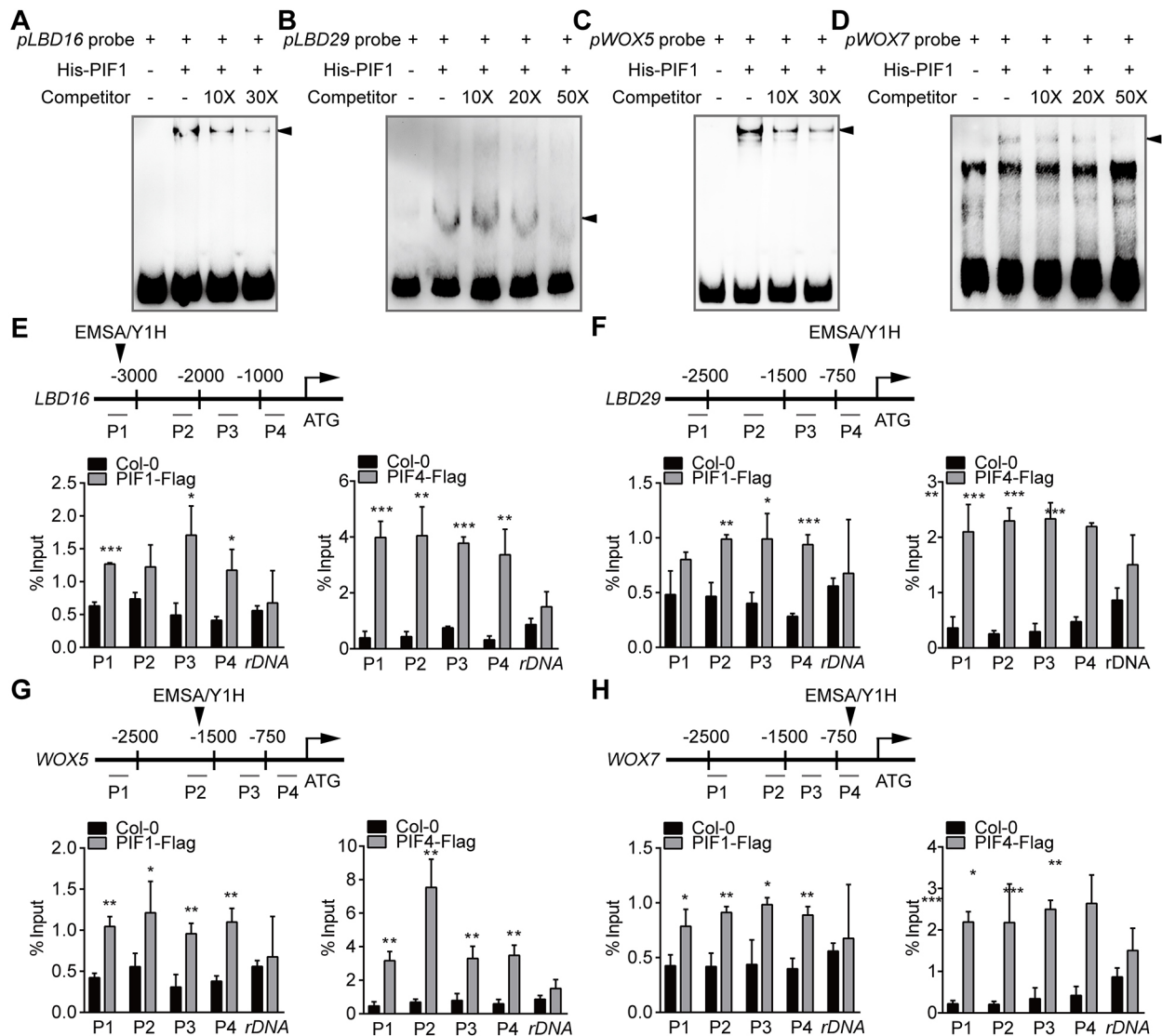


Fig. 8. PIFs directly bind the promoters of the *LBD16*, *LBD29*, *WOX5* and *WOX7* genes *in vitro* and *in vivo*. (A–D) EMSA showing that His-PIF1 recombinant proteins bind to biotin-labeled probes of the *LBD16*, *LBD29*, *WOX5* and *WOX7* promoters. Black arrowheads indicate the shifted bands. (E–H) ChIP assays of *LBD16*, *LBD29*, *WOX5* and *WOX7* in 8-day-old Col-0, *PIF1-Flag* or *PIF4-Flag* seedlings grown under red light for 2 days and then transferred to darkness for 6 days. Data are derived from three biological replicates. Data are mean \pm s.d. The asterisks represent significant differences compared with the wild type according to an unpaired two-tailed Student's *t*-test (* $P < 0.05$; ** $P < 0.01$; *** $P < 0.001$).

responsive to auxin signaling but also can be directly regulated by PIFs.

As PIFs could directly activate auxin biosynthesis, transport and TFs for HAR priming, these essential skotomorphogenesis regulators essentially function as coordinators of HAR formation. Multiple regulatory points of HARs controlled by a single type of TF reflect that HAR formation is an orchestrated process. Such regulation of HARs by PIFs might facilitate the tight coupling of HAR formation and skotomorphogenesis, which ensures the development of ARs from the hypocotyls embedded in soil.

PIFs are responsible for the divergence in the initiation of LRs, HARs and wound-induced ARs

We have reported that the initiation of LRs and that of HARs share common regulatory components, including the IAA14-ARF7/19 module, *AUX1*, *LAX3*, *LBD16*, *LBD29*, *WOX5* and *WOX7*. However, LRs are developed programmatically from roots, whereas HARs emerge from hypocotyls in response to

environmental stimuli. Such a difference suggests that there must be a point of divergence in the regulatory mechanism underlying HAR and LR formation. We found that PIFs do not affect LR development, although they do contribute to the regulation of auxin biosynthesis, auxin transport and activation of *LBD16*, *LBD29*, *WOX5* and *WOX7*. The different requirements of PIFs in HAR and LR formation explain the divergence of HAR and LR development. The most likely reason for the different requirements of PIFs could be that *PIF* expression can be highly induced in hypocotyls but be barely induced in roots.

YUC2, *YUC6*, *LBD16*, *LBD29*, *WOX5* and *WOX7* have also been reported to be involved in AR formation in leaf explants (Chen et al., 2016; Hu and Xu, 2016; Sheng et al., 2017), and our results showed that PIFs are also required for this process. This evidence demonstrated that HARs and wound-induced ARs share similar regulatory mechanisms, which might be mediated by PIFs. However, the involvement of PIFs in HAR and wound-induced AR formation is different, given that *pirf* does not develop any

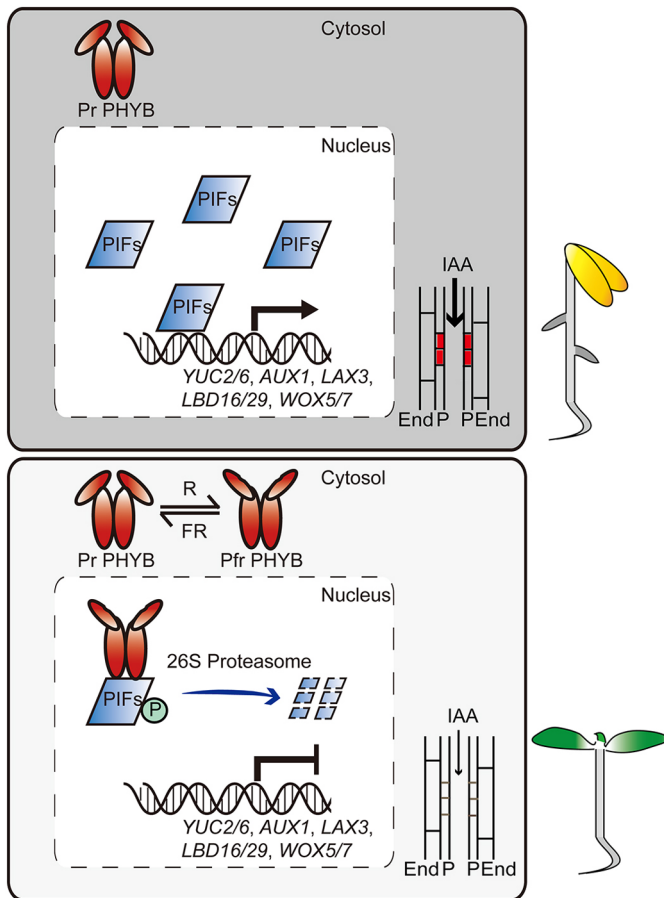


Fig. 9. Proposed model illustrating the function of PIFs in HAR formation in wild type. In the dark, PIFs localize in the nucleus and activate *YUC2*, *YUC6*, *AUX1*, *LAX3*, *LBD16*, *LBD29*, *WOX5* and *WOX7* expression, leading to auxin biosynthesis and auxin influx into pericycle cells, and promoting root primordium gene expression to induce HAR formation. Light induces conformational changes in phytochromes such that they are in the active form and are subsequently translocated into the nucleus. The phytochrome proteins then physically interact with PIFs, which results in the phosphorylation of PIF proteins. The phosphorylated forms of PIFs, which repress the expression of these genes, are subsequently degraded by the 26S proteasome, preventing auxin from accumulating in pericycle cells and inhibiting HAR formation.

HARs but that leaf explants still produce ARs, albeit to a lesser degree than the wild type. These differences might also be attributed to low expression of *PIFs* in leaf explants.

MATERIALS AND METHODS

Plant materials, growth conditions and tissue culture

All of the *A. thaliana* lines used in this work are in the Col-0 background. The *pif1-1*, *pif3-7*, *pif4-2*, *pif5-3*, *phyB-9*, *pifq* and *cop1-6* mutants were obtained from Dr Hongtao Liu (Chinese Academy of Sciences Center for Excellence in Molecular Plant Sciences, Shanghai, China). *phyB pifq* were kindly provided by P. Quail (University of California, Berkeley, USA), and *yuc1 yuc4*, *yuc2 yuc6*, *aux1* (GABI_459H07), *lax2* (GABI_345D11), *lax3* (SAIL_855_F07), *lax2 lax3* and *WOX5_{pro}:GUS* were obtained from Dr. Lin Xu (Chinese Academy of Sciences Center for Excellence in Molecular Plant Sciences, Shanghai, China) (Cheng et al., 2006). The *aux1* mutant was crossed with *lax3* to generate the *aux1 lax3* double mutant. The *DR5:GUS* plant was crossed with *pifq* to generate the *DR5:GUS/pifq* reporter line. The *WOX5_{pro}:GUS* plant was crossed with *pifq* to generate the *WOX5_{pro}:GUS/pifq* reporter line. The full-length coding DNA sequences (CDSs) of *PIF1*, *PIF3*, *PIF4* and *PIF5* were cloned into an entry vector (pDONR/Zeo) and subsequently recombined into a destination vector pCambia1300-gateway

(Liang et al., 2018) to generate *35S:PIF1-Flag (PIF1-OX)*, *35S:PIF3-Flag (PIF3-OX)*, *35S:PIF4-Flag (PIF4-OX)* and *35S:PIF5-Flag (PIF5-OX)*, respectively. For construction of the *YUC2_{pro}:GUS*, *YUC6_{pro}:GUS*, *AUX1_{pro}:GUS* and *LAX3_{pro}:GUS* transgenic plants in the wild-type and *pifq* mutant background, the *YUC2* promoter (3 kb), the *YUC6* promoter (3.3 kb), the *AUX1* promoter (2.6 kb) upstream of the translation start site plus the first exon and intron (270 bp) (Marchant et al., 1999) and the *LAX3* promoter (1.9 kb) plus a partial segment of the first exon (132 bp), were subcloned into pRR00 vectors, respectively. For construction of the *LBD16_{pro}:LBD16-GUS* transgenic plants and the *LBD16_{pro}:LBD16-GFP* transgenic plants in wild-type and *pifq* mutant backgrounds, the *LBD16* promoter (4.8 kb) plus full-length gene sequence was subcloned into pCambia1300 and pCambia1301 vectors, respectively (Hu and Xu, 2016). *AUX1_{pro}:AUX1-GFP* and *LAX3_{pro}:LAX3-GFP* constructs were generated according to previous studies (Swarup et al., 2004, 2008). For construction of *35S:AUX1* transgenic plants in the *pifq* mutant background, the CDS of *AUX1* was cloned and subsequently inserted into a pCambia1301 vector. Stock seeds of *pif1 pif3* (N66045), *pif1 pif4* (N68811), *pif1 pif5* (N68094), *pif3 pif4* (N66046), *pif3 pif5* (N68812), *pif1 pif3 pif4* (N66500), *pif1 pif3 pif5* (N66047), *pif1 pif4 pif5* (N68095), *pif3 pif4 pif5* (N66048) and *yuc5 yuc8 yuc9* (N69942) were purchased from the European Arabidopsis Stock Centre. T-DNA lines of *yuc2* (N659779) and *yuc6* (N663363) were obtained from AraShare (China).

To initiate the formation of ARs from hypocotyls, seeds were surface sterilized, stratified for 1 day at 4°C and then sown on plates containing half-strength Murashige and Skoog (1/2 MS) media, which were incubated in white light for 6 h and then transferred to red light (40 $\mu\text{mol}\cdot\text{m}^{-2}\cdot\text{sec}^{-1}$) or darkness for the required duration as indicated. The numbers of HARs were determined using a dissecting microscope. Similarly, induction of the formation ARs from leaf explants was performed as previously described (Li et al., 2021).

Immunoblot assays

Immunoblot assays were performed as previously described (Liu et al., 2008). For immunoblots, the hypocotyls of 5-day-old seedlings were harvested and ground in liquid nitrogen. The samples were subsequently solubilized with NEB buffer, after which the resulting protein extracts were centrifuged at 14,000 g for 10 min. The supernatants were collected, mixed with 5 \times SDS-PAGE loading buffer and then analyzed using SDS-PAGE and immunoblotting with anti-Flag (Sigma-Aldrich), anti-actin antibodies (Sangon) and anti-IAA14 antibodies (Li et al., 2021).

Trypan Blue staining

Trypan Blue staining was performed as previously described (Zhao et al., 2018). Briefly, seedlings were submerged in Trypan Blue staining solution (30 ml of ethanol, 10 g of phenol, 10 ml of H₂O, 10 ml of glycerol, 10 ml of lactic acid and 10 mg of Trypan Blue) and boiled for 2-3 min, after which they were allowed to cool to room temperature for 1 h. The stained seedlings were then decolorized in chloral hydrate solution. Trypan blue staining was observed using a Nikon Eclipse Ni light microscope.

Histochemical analysis and microscopy

Seedlings were submerged and maintained in GUS staining solution [2 mM K₄Fe(CN)₆, 2 mM K₃Fe(CN)₆, 0.5 mg ml⁻¹ X-Gluc, 10 mM EDTA, 0.1% Triton X-100, 50 mM Na₂HPO₄-NaH₂PO₄ (pH 7.0)] at 37°C for 5-10 h. The stained seedlings were then decolorized in 70% (v/v) ethanol and incubated in chloral hydrate solution (200 g of chloral hydrate, 20 g of glycerol and 50 ml of water) at room temperature for ~12 h to induce tissue transparency (Liu et al., 2014). GUS staining was observed using a Nikon Eclipse Ni light microscope.

Confocal microscopy was performed using a Leica TCS SP8 confocal laser scanning microscope. Briefly hypocotyls of the seeds grown on 1/2 MS medium in the dark for 6 days were analyzed with an excitation wavelength of 488 nm and an emission wavelength of 505-550 nm. For propidium iodide (PI) staining, seedlings were incubated in a fresh solution with 15 mM (10 mg/ml) PI dissolved in water in the dark for 2 h, followed by three washes with water. The fluorescence excitation and emission wavelengths of PI were 561 nm and 610-630 nm, respectively.

RNA isolation and qRT-PCR analysis

For gene expression analysis, total RNA was extracted from the hypocotyls of seedlings grown in the dark. RNA isolation and qRT-PCR analysis were performed according to previously described methods (Gao et al., 2017) in conjunction with gene-specific primers (Table S1). The *UBC21* gene was used as an internal control, and at least three biological replicates were tested.

Y1H assays

Y1H assays were performed using a Matchmaker Gold Yeast One-Hybrid System Kit (Clontech) according to the manufacturer's protocol. Fragments of *AUX1*, *LBD16*, *LBD29*, *WOX5* and *WOX7* promoters containing PBE-box, G-box, E-box or mutant E-box motifs were synthesized, annealed and ligated into pAbAi vectors digested with XhoI to generate pAbAi-pAUX1-P3, pAbAi-pAUX1-mP3, pAbAi-pLBD16-P1, pAbAi-pLBD29-P2, pAbAi-pWOX5-P2 and pAbAi-pWOX7-P3. Similarly, the CDSs of *PIF1*, *PIF3*, *PIF4* and *PIF5* were subcloned and ligated into pGADT7 vectors. The oligonucleotide sequences of the promoters and the primers used to clone the CDSs of *PIF1*, *PIF3*, *PIF4* and *PIF5* are listed in Table S1. The pAbAi vectors were linearized and transformed into Y1H Gold yeast strains. Transformants were selected on SD/-Ura dropout plates, and the minimal concentration of AbA that completely suppressed strain growth was identified. The pGADT7 constructs were subsequently transformed into Y1H Gold strain cells harboring different pAbAi vectors, after which the transformants were screened on SD/-Leu plants with AbA.

Y2H assays

The CDS of *IAA14* and cDNA fragments without the activation domain of ARF19 (ARF19-AD, of which amino acids 550 to 724 were deleted) were subcloned and inserted into pGBKT7 vectors, and the CDSs of *PIF1*, *PIF3*, *PIF4* and *PIF5* were subcloned and inserted into pGADT7 vectors. For interaction analysis, two combinatorial constructs were co-transformed into the yeast strain AH109 via the lithium acetate transformation procedure, as described in the Yeast Protocols Handbook (Clontech). Empty pGADT7 or pGBKT7 vectors were used as negative controls. The transformants were grown on SD/-Leu-Trp-His-Ade dropout plates.

Dual-LUC assays

For transient transcription dual-LUC assays of *A. thaliana* protoplasts, mesophyll protoplasts were isolated from 4-week-old Col-0 plants grown under long-day conditions (16 h of light/8 h of darkness). The promoters of *YUC2*, *YUC6*, *AUX1* and *LAX3* were cloned and inserted into pGreenII 0800-LUC vectors as reporters, and the CDSs of *PIF1*, *PIF3*, *PIF4* and *PIF5* were cloned and inserted into pA7 vectors as effectors. Protoplast isolation and polyethylene glycol (PEG) transformation were carried out as described previously (Yoo et al., 2007). Approximately 2×10^4 protoplasts were transfected with 10 μ g of reporter DNA and 10 μ g of effector DNA and then incubated in red light for 16 h. Then, these protoplasts were harvested by centrifugation for dual-LUC assays with a Dual-Luciferase Reporter system (Promega) according to the manufacturer's instructions. The REN activity for each reaction was used as an internal control.

EMSAs

To generate recombinant His-PIF1 proteins, the CDS of PIF1 was inserted into the pETDuet-M2 vector and expressed in the *Escherichia coli* Rosetta (DE3) strain. For probes, biotin-labeled complementary oligonucleotides of the *YUC2*, *YUC6*, *AUX1*, *LAX3*, *LBD16*, *LBD29*, *WOX5* and *WOX7* promoter fragments containing PBE boxes, G boxes or E boxes were synthesized and annealed. EMSAs were performed according to the manufacturer's instructions of the LightShift Chemiluminescent EMSA Kit (Thermo Fisher Scientific). The migration of the biotin-labeled probe was determined using a Chemiluminescent Nucleic Acid Detection Module (Thermo Fisher Scientific) and a Tanon-5200 Chemiluminescent Imaging System (Tanon Science and Technology). The oligonucleotide sequences are listed in Table S1.

ChIP assays

ChIP experiments were performed as described previously (Liang et al., 2018) by using transgenic plants that expressed *PIF1-Flag* or *PIF4-Flag*,

and that were grown under red light for 2 days and then transferred to darkness for 6 days. The seedlings were crosslinked with 1% formaldehyde (Sigma-Aldrich) under vacuum, which was stopped with glycine. The seedlings were then ground and homogenized in extraction buffer 1 (0.4 M sucrose, 10 mM Tris-HCl (pH 8.0), 5 mM β -mercaptoethanol, 0.1 mM phenylmethylsulfonyl fluoride (PMSF) and 1X cOmplete Protease Inhibitor Cocktail tablets (Roche)). Nuclei were precipitated by centrifugation at 2000 g for 20 min, washed with extraction buffer 2 [0.25 M sucrose, 10 mM Tris-HCl (pH 8.0), 10 mM MgCl₂, 1% Triton X-100, 5 mM β -mercaptoethanol, 0.1 mM PMSF and 1X cOmplete Protease Inhibitor Cocktail tablets (Roche)] and then lysed in nuclear lysis buffer [50 mM Tris-HCl (pH 8.0), 10 mM EDTA, 1% SDS, 0.1 mM PMSF and 1X cOmplete Protease Inhibitor Cocktail tablets (Roche)]. The chromatin was sheared by sonication, after which the chromatin solution was diluted 10-fold with ChIP dilution buffer [1.1% Triton X-100, 16.7 mM Tris-HCl (pH 8.0), 1.2 mM EDTA, 167 mM NaCl, 0.1 mM PMSF and 1 \times cOmplete Protease Inhibitor Cocktail tablets (Roche)]. Anti-Flag Sepharose and the chromatin solution were mixed together and then incubated at 4°C overnight. The beads were washed sequentially with a low-salt buffer [150 mM NaCl, 0.1% SDS, 1% Triton X-100, 2 mM EDTA and 20 mM Tris-HCl (pH 8.0)], a high-salt buffer [500 mM NaCl, 0.1% SDS, 1% Triton X-100, 2 mM EDTA and 20 mM Tris-HCl (pH 8.0)], LiCl washing buffer [0.25 M LiCl, 1% NP40, 1% sodium deoxycholate, 1 mM EDTA and 10 mM Tris-HCl (pH 8.0)] and TE buffer [10 mM Tris-HCl (pH 8.0) and 1 mM EDTA]. The resulting immunocomplexes were eluted with elution buffer (1% SDS and 0.1 M NaHCO₃) and the crosslinks reversed overnight at 65°C. The mixture was subsequently treated with Proteinase K, after which the precipitated DNA was recovered and subjected to qPCR. The primers used in the ChIP-qPCR experiments are listed in Table S1.

Acknowledgements

We thank H. T. Liu, L. Xu and P. Quail for the *Arabidopsis* seeds. We thank Y. R. Wu for providing the pAbAi vector. We thank J. W. Wang for providing the pRR00 vector.

Competing interests

The authors declare no competing or financial interests.

Author contributions

Conceptualization: Q.-Q.L., D.-Y.C.; Methodology: Q.-Q.L.; Validation: Q.-Q.L.; Formal analysis: Q.-Q.L.; Investigation: Q.-Q.L., Z.Z., C.-X.Z., Y.-L.W., C.-B.L., J.-C.W., M.-L.H., Q.-X.W.; Resources: D.-Y.C.; Writing - original draft: Q.-Q.L., D.-Y.C.; Supervision: D.-Y.C.; Project administration: D.-Y.C.; Funding acquisition: D.-Y.C.

Funding

This research was supported by the National Natural Science Foundation of China (31930024), the Chinese Academy of Sciences (XDB27010103) and the Newton Fund (NAF1R1201264).

Peer review history

The peer review history is available online at <https://journals.biologists.com/dev/article-lookup/doi/10.1242/dev.200362>

References

- Bae, G. and Choi, G. (2008). Decoding of light signals by plant phytochromes and their interacting proteins. *Annu. Rev. Plant Biol.* **59**, 281-311. doi:10.1146/annurev-arplant.59.032607.092859
- Bellini, C., Pacurar, D. I. and Perrone, I. (2014). Adventitious roots and lateral roots: similarities and differences. *Annu. Rev. Plant Biol.* **65**, 639-666. doi:10.1146/annurev-arplant-050213-035645
- Blakeslee, J. J., Peer, W. A. and Murphy, A. S. (2005). Auxin transport. *Curr. Opin. Plant Biol.* **8**, 494-500. doi:10.1016/j.pbi.2005.07.014
- Boerjan, W., Cervera, M. T., Delarue, M., Beeckman, T., Dewitte, W., Bellini, C., Caboche, M., Van Onckelen, H., Van Montagu, M. and Inzé, D. (1995). Superroot, a recessive mutation in *Arabidopsis*, confers auxin overproduction. *Plant Cell* **7**, 1405-1419.
- Castillon, A., Shen, H. and Huq, E. (2007). Phytochrome Interacting Factors: central players in phytochrome-mediated light signaling networks. *Trends Plant Sci.* **12**, 514-521. doi:10.1016/j.tplants.2007.10.001

- Chen, L., Tong, J., Xiao, L., Ruan, Y., Liu, J., Zeng, M., Huang, H., Wang, J.-W. and Xu, L. (2016). YUCCA-mediated auxin biogenesis is required for cell fate transition occurring during de novo root organogenesis in Arabidopsis. *J. Exp. Bot.* **67**, 4273-4284. doi:10.1093/jxb/erw213
- Cheng, Y., Dai, X. and Zhao, Y. (2006). Auxin biosynthesis by the YUCCA flavin monooxygenases controls the formation of floral organs and vascular tissues in Arabidopsis. *Genes Dev.* **20**, 1790-1799. doi:10.1101/gad.1415106
- Delbarre, A., Muller, P., Imhoff, V. and Guern, J. (1996). Comparison of mechanisms controlling uptake and accumulation of 2,4-dichlorophenoxy acetic acid, naphthalene-1-acetic acid, and indole-3-acetic acid in suspension-cultured tobacco cells. *Planta* **198**, 532-541. doi:10.1007/BF00262639
- Della Rovere, F., Fattorini, L., D'Angeli, S., Velocchia, A., Falasca, G. and Altamura, M. M. (2013). Auxin and cytokinin control formation of the quiescent centre in the adventitious root apex of Arabidopsis. *Ann. Bot.* **112**, 1395-1407. doi:10.1093/aob/mct215
- Della Rovere, F., Fattorini, L., D'Angeli, S., Velocchia, A., Del Duca, S., Cai, G., Falasca, G. and Altamura, M. M. (2015). Arabidopsis SHR and SCR transcription factors and AUX1 auxin influx carrier control the switch between adventitious rooting and xylogenesis in planta and in vitro cultured thin cell layers. *Ann. Bot.* **115**, 617-628. doi:10.1093/aob/mcu258
- Di, D.-W., Wu, L., Zhang, L., An, C.-W., Zhang, T.-Z., Luo, P., Gao, H.-H., Kriechbaumer, V. and Guo, G.-Q. (2016). Functional roles of Arabidopsis CKRC2/YUCCA8 gene and the involvement of PIF4 in the regulation of auxin biosynthesis by cytokinin. *Sci. Rep.* **6**, 36866. doi:10.1038/srep36866
- Gao, Y.-Q., Chen, J.-G., Chen, Z.-R., An, D., Lv, Q.-Y., Han, M.-L., Wang, Y.-L., Salt, D. E. and Chao, D.-Y. (2017). A new vesicle trafficking regulator CTL1 plays a crucial role in ion homeostasis. *PLoS Biol.* **15**, e2002978. doi:10.1371/journal.pbio.2002978
- Grones, P. and Friml, J. (2015). Auxin transporters and binding proteins at a glance. *J. Cell Sci.* **128**, 1-7. doi:10.1242/jcs.159418
- Gutierrez, L., Bussell, J.-D., Pacurar, D. I., Schwambach, J., Pacurar, M. and Bellini, C. (2009). Phenotypic plasticity of adventitious rooting in Arabidopsis is controlled by complex regulation of AUXIN RESPONSE FACTOR transcripts and microRNA abundance. *Plant Cell* **21**, 3119-3132. doi:10.1105/tpc.108.064758
- Gutierrez, L., Mongelard, G., Flokova, K., Pacurar, D. I., Novak, O., Staswick, P., Kowalczyk, M., Pacurar, M., Demailly, H., Geiss, G. et al. (2012). Auxin controls Arabidopsis adventitious root initiation by regulating jasmonic acid homeostasis. *Plant Cell* **24**, 2515-2527. doi:10.1105/tpc.112.099119
- Hornitschek, P., Kohnen, M. V., Lorrain, S., Rougemont, J., Ljung, K., Lopez-Vidriero, I., Franco-Zorrilla, J. M., Solano, R., Trevisan, M., Pradervand, S. et al. (2012). Phytochrome interacting factors 4 and 5 control seedling growth in changing light conditions by directly controlling auxin signaling. *Plant J.* **71**, 699-711. doi:10.1111/j.1365-313X.2012.05033.x
- Hu, X. and Xu, L. (2016). Transcription factors WOX11/12 directly activate WOX5/7 to promote root primordia initiation and organogenesis. *Plant Physiol.* **172**, 2363-2373. doi:10.1104/pp.16.01067
- Lakehal, A. and Bellini, C. (2019). Control of adventitious root formation: insights into synergistic and antagonistic hormonal interactions. *Physiol. Plant.* **165**, 90-100. doi:10.1111/pp.12823
- Lakehal, A., Chaabouni, S., Cavel, E., Le Hir, R., Ranjan, A., Raneshan, Z., Novak, O., Pacurar, D. I., Perrone, I., Jobert, F. et al. (2019). A molecular framework for the control of adventitious rooting by TIR1/AFB2-Aux/IAA-dependent auxin signaling in Arabidopsis. *Mol. Plant* **12**, 1499-1514. doi:10.1016/j.molp.2019.09.001
- Lee, H. W., Cho, C., Pandey, S. K., Park, Y., Kim, M.-J. and Kim, J. (2019). LBD16 and LBD18 acting downstream of ARF7 and ARF19 are involved in adventitious root formation in Arabidopsis. *BMC Plant Biol.* **19**, 46. doi:10.1186/s12870-019-1659-4
- Leivar, P., Monte, E., Al-Sady, B., Carle, C., Storer, A., Alonso, J. M., Ecker, J. R. and Quail, P. H. (2008). The Arabidopsis phytochrome-interacting factor PIF7, together with PIF3 and PIF4, regulates responses to prolonged red light by modulating phyB levels. *Plant Cell* **20**, 337-352. doi:10.1105/tpc.107.052142
- Li, L., Ljung, K., Breton, G., Schmitz, R. J., Pruneda-Paz, J., Cowing-Zitron, C., Cole, B. J., Ivans, L. J., Pedmale, U. V., Jung, H. S. et al. (2012). Linking photoreceptor excitation to changes in plant architecture. *Genes Dev.* **26**, 785-790. doi:10.1101/gad.187849.112
- Li, Q. Q., Zhang, Z., Wang, Y. L., Zhong, L. Y., Chao, Z. F., Gao, Y. Q., Han, M. L., Xu, L. and Chao, D. Y. (2021). Phytochrome B inhibits darkness-induced hypocotyl adventitious root formation by stabilizing IAA14 and suppressing ARF7 and ARF19. *Plant J.* **105**, 1689-1702. doi:10.1111/tpj.15142
- Liang, T., Mei, S., Shi, C., Yang, Y., Peng, Y., Ma, L., Wang, F., Li, X., Huang, X., Yin, Y. et al. (2018). UVR8 interacts with BES1 and BIM1 to regulate transcription and photomorphogenesis in Arabidopsis. *Dev. Cell* **44**, 512-523. doi:10.1016/j.devcel.2017.12.028
- Liu, H., Yu, X., Li, K., Klejnot, J., Yang, H., Lisiero, D. and Lin, C. (2008). Photoexcited CRY2 interacts with CIB1 to regulate transcription and floral initiation in Arabidopsis. *Science* **322**, 1535-1539. doi:10.1126/science.1163927
- Liu, J., Sheng, L., Xu, Y., Li, J., Yang, Z., Huang, H. and Xu, L. (2014). WOX11 and 12 are involved in the first-step cell fate transition during de novo root organogenesis in Arabidopsis. *Plant Cell* **26**, 1081-1093. doi:10.1105/tpc.114.122887
- Lorrain, S., Allen, T., Duek, P. D., Whitelam, G. C. and Fankhauser, C. (2008). Phytochrome-mediated inhibition of shade avoidance involves degradation of growth-promoting bHLH transcription factors. *Plant J.* **53**, 312-323. doi:10.1111/j.1365-313X.2007.03341.x
- Marchant, A., Kargul, J., May, S. T., Muller, P., Delbarre, A., Perrot-Rechenmann, C. and Bennett, M. J. (1999). AUX1 regulates root gravitropism in Arabidopsis by facilitating auxin uptake within root apical tissues. *EMBO J.* **18**, 2066-2073. doi:10.1093/emboj/18.8.2066
- Ni, W., Xu, S.-L., Chalkley, R. J., Pham, T. N., Guan, S., Maltby, D. A., Burlingame, A. L., Wang, Z.-Y. and Quail, P. H. (2013). Multisite light-induced phosphorylation of the transcription factor PIF3 is necessary for both its rapid degradation and concomitant negative feedback modulation of photoreceptor phyB levels in Arabidopsis. *Plant Cell* **25**, 2679-2698. doi:10.1105/tpc.113.112342
- Pucciariello, O., Legris, M., Costigliolo Rojas, C., Iglesias, M. J., Hernandez, C. E., Dezar, C., Vazquez, M., Yanovsky, M. J., Finlayson, S. A., Prat, S. et al. (2018). Rewiring of auxin signaling under persistent shade. *Proc. Natl. Acad. Sci. USA* **115**, 5612-5617. doi:10.1073/pnas.1721110115
- Shen, H., Zhu, L., Castillon, A., Majee, M., Downie, B. and Huq, E. (2008). Light-induced phosphorylation and degradation of the negative regulator PHYTOCHROME-INTERACTING FACTOR1 from Arabidopsis depend upon its direct physical interactions with photoactivated phytochromes. *Plant Cell* **20**, 1586-1602. doi:10.1105/tpc.108.060020
- Sheng, L., Hu, X., Du, Y., Zhang, G., Huang, H., Scheres, B. and Xu, L. (2017). Non-canonical WOX11-mediated root branching contributes to plasticity in Arabidopsis root system architecture. *Development* **144**, 3126-3133.
- Simon, S., Skupa, P., Viaeane, T., Zwiewka, M., Tejos, R., Klíma, P., Černá, M., Rolčík, J., De Rycke, R., Moreno, I. et al. (2016). PIN6 auxin transporter at endoplasmic reticulum and plasma membrane mediates auxin homeostasis and organogenesis in Arabidopsis. *New Phytol.* **211**, 65-74. doi:10.1111/nph.14019
- Smetana, O., Mäkilä, R., Lyu, M., Amiryousefi, A., Sánchez Rodríguez, F., Wu, M.-F., Solé-Gil, A., Leal Gavarrón, M., Siligato, R., Miyashima, S. et al. (2019). High levels of auxin signalling define the stem-cell organizer of the vascular cambium. *Nature* **565**, 485-489. doi:10.1038/s41586-018-0837-0
- Sorin, C., Bussell, J. D., Camus, I., Ljung, K., Kowalczyk, M., Geiss, G., McKhann, H., Garcion, C., Vaucheret, H., Sandberg, G. et al. (2005). Auxin and light control of adventitious rooting in Arabidopsis require ARGONAUTE1. *Plant Cell* **17**, 1343-1359. doi:10.1105/tpc.105.031625
- Soy, J., Leivar, P., Gonzalez-Schain, N., Sentandreu, M., Prat, S., Quail, P. H. and Monte, E. (2012). Phytochrome-imposed oscillations in PIF3 protein abundance regulate hypocotyl growth under diurnal light/dark conditions in Arabidopsis. *Plant J.* **71**, 390-401.
- Sukumar, P., Maloney, G. S. and Muday, G. K. (2013). Localized Induction of the ATP-Binding Cassette B19 Auxin Transporter Enhances Adventitious Root Formation in Arabidopsis. *Plant Physiol.* **162**, 1392-1405. doi:10.1104/pp.113.217174
- Sun, J., Qi, L., Li, Y., Chu, J. and Li, C. (2012). PIF4-mediated activation of YUCCA8 expression integrates temperature into the auxin pathway in regulating Arabidopsis hypocotyl growth. *PLoS Genet.* **8**, e1002594. doi:10.1371/journal.pgen.1002594
- Swarup, R. and Peret, B. (2012). AUX/LAX family of auxin influx carriers-an overview. *Front. Plant Sci.* **3**, 225. doi:10.3389/fpls.2012.00225
- Swarup, R., Kargul, J., Marchant, A., Zadić, D., Rahman, A., Mills, R., Yemm, A., May, S., Williams, L., Millner, P. et al. (2004). Structure-function analysis of the presumptive Arabidopsis auxin permease AUX1. *Plant Cell* **16**, 3069-3083. doi:10.1105/tpc.104.024737
- Swarup, K., Benkova, E., Swarup, R., Casimiro, I., Peret, B., Yang, Y., Parry, G., Nielsen, E., De Smet, I., Vanneste, S. et al. (2008). The auxin influx carrier LAX3 promotes lateral root emergence. *Nat. Cell Biol.* **10**, 946-954. doi:10.1038/ncb1754
- Ursache, R., Miyashima, S., Chen, Q., Vaten, A., Nakajima, K., Carlsbecker, A., Zhao, Y., Helariutta, Y. and Dettmer, J. (2014). Tryptophan-dependent auxin biosynthesis is required for HD-ZIP III-mediated xylem patterning. *Development* **141**, 1250-1259. doi:10.1242/dev.103473
- Velocchia, A., Fattorini, L., Della Rovere, F., Sofo, A., D'Angeli, S., Betti, C., Falasca, G. and Altamura, M. M. (2016). Ethylene and auxin interaction in the control of adventitious rooting in Arabidopsis thaliana. *J. Exp. Bot.* **67**, 6445-6458. doi:10.1093/jxb/erw415
- Verstraeten, I., Schotte, S. and Geelen, D. (2014). Hypocotyl adventitious root organogenesis differs from lateral root development. *Front. Plant Sci.* **5**, 495. doi:10.3389/fpls.2014.00495
- Xu, L. (2018). De novo root regeneration from leaf explants: wounding, auxin, and cell fate transition. *Curr. Opin. Plant Biol.* **41**, 39-45. doi:10.1016/j.pbi.2017.08.004

- Yoo, S. D., Cho, Y. H. and Sheen, J.** (2007). Arabidopsis mesophyll protoplasts: a versatile cell system for transient gene expression analysis. *Nat. Protoc.* **2**, 1565-1572. doi:10.1038/nprot.2007.199
- Zhang, Y., Mayba, O., Pfeiffer, A., Shi, H., Tepperman, J. M., Speed, T. P. and Quail, P. H.** (2013). A quartet of PIF bHLH factors provides a transcriptionally centered signaling hub that regulates seedling morphogenesis through differential expression-patterning of shared target genes in Arabidopsis. *PLoS Genet.* **9**, e1003244. doi:10.1371/journal.pgen.1003244
- Zhao, Y., Christensen, S., Fankhauser, C., Cashman, J., Cohen, J., Weigel, D. and Chory, J.** (2001). A role for flavin monooxygenase-like enzymes in auxin biosynthesis. *Science* **291**, 306-309. doi:10.1126/science.291.5502.306
- Zhao, Y., Luo, L., Xu, J., Xin, P., Guo, H., Wu, J., Bai, L., Wang, G., Chu, J., Zuo, J. et al.** (2018). Malate transported from chloroplast to mitochondrion triggers production of ROS and PCD in Arabidopsis thaliana. *Cell Res.* **28**, 1. doi:10.1038/cr.2017.154

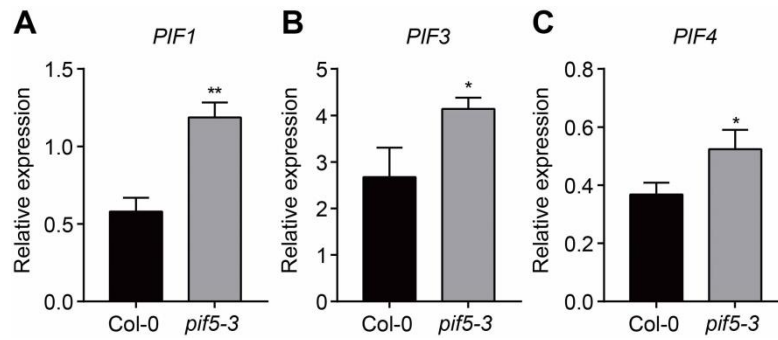


Fig. S1. Expression of *PIF* genes in *pif5-3*.

(A-C) qRT-PCR results of *PIF1* (A), *PIF3* (B) and *PIF4* (C) gene expression in hypocotyls of plants grown in darkness for 5 days. Data are derived from three biological replicates. Data are represented as mean \pm s.d. The asterisks represent significant differences compared with the wild type according to Student's *t* tests (*, $P < 0.05$; **, $P < 0.01$).

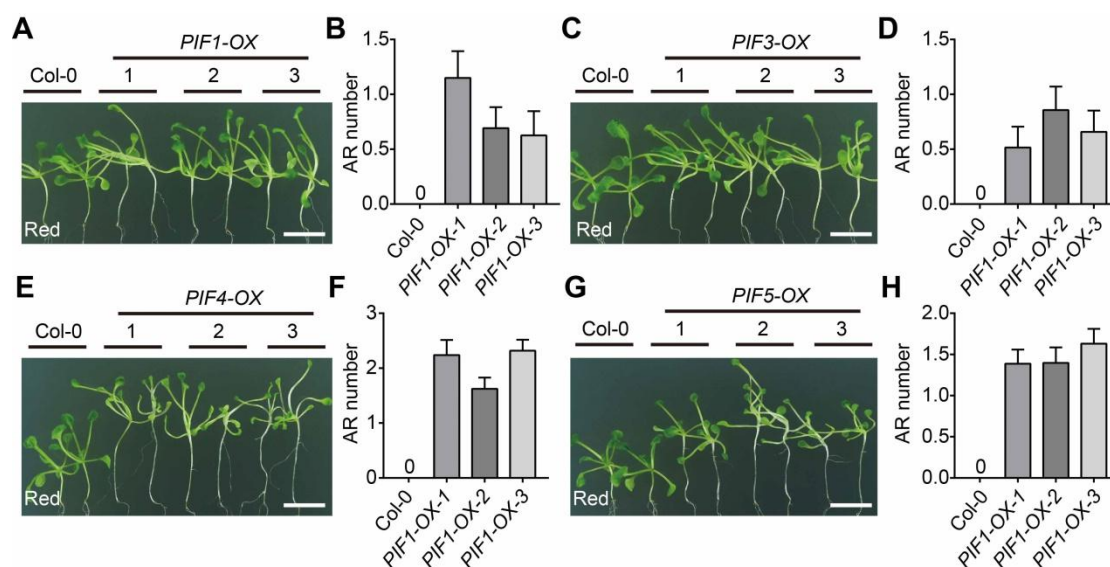


Fig. S2. Overexpression of *PIFs* promotes HAR formation under red light.

(A) Representative images of 14-day-old seedlings of Col-0 and three independent lines of the *PIF1* overexpression (*PIF1-OX*) lines (#1, #2, #3) grown in red light. (B) Quantification of HAR numbers of the plants in (A). (C) Representative images of 14-day-old seedlings of Col-0 and three independent lines of the *PIF3* overexpression (*PIF3-OX*) lines (#1, #2, #3) grown in red light. (D) Quantification of HAR numbers of the plants in (C). (E) Representative images of 14-day-old seedlings of Col-0 and three independent lines of the *PIF4* overexpression (*PIF4-OX*) lines (#1, #2, #3) grown in red light. (F) Quantification of HAR numbers of the plants in (E). (G) Representative images of 14-day-old seedlings of Col-0 and three independent lines of the *PIF5* overexpression (*PIF5-OX*) lines (#1, #2, #3) grown in red light. (H), Quantification of HAR numbers of the plants in (G). The data are from three independent biological replicates, with each replicate including 12 seedlings. Data are represented as mean \pm s.e.m. The white scale bars represent 1 cm.

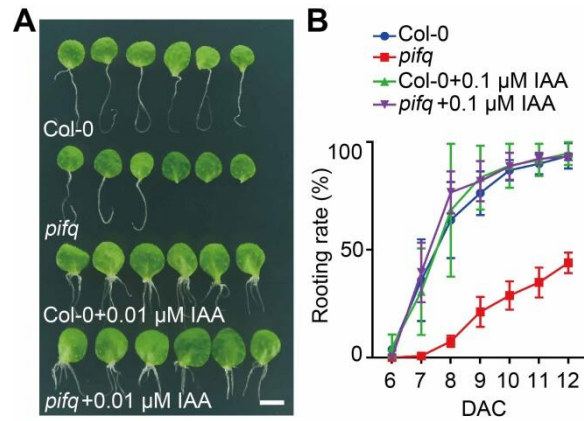


Fig. S3. PIFs are involved in the adventitious rooting of leaf explants.

(A) Formation of ARs in leaf explants from Col-0 and *pifq* seedlings grown on B5 media supplemented with or without 0.01 μM IAA. The white scale bars represent 5 mm. (B) Quantification of the degree of rooting of the plants in (A). Data are derived from three biological replicates. Data are represented as mean \pm s.d.

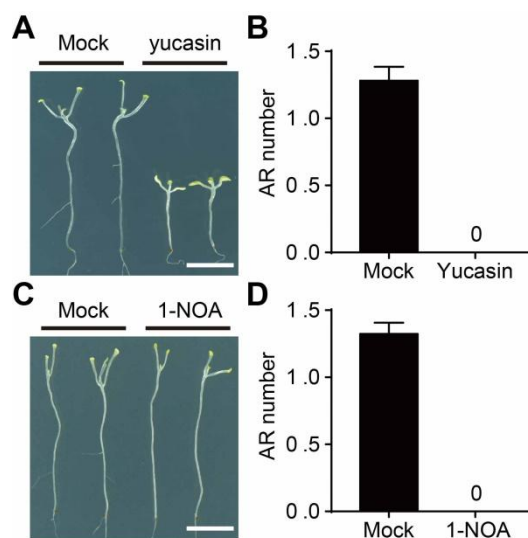


Fig. S4. Auxin biosynthesis and transport are essential for HAR formation.

(A) Representative images of 14-day-old Col-0 seedlings grown on 1/2 MS media supplemented without or with 100 μ M yucasin in the dark. (B) Quantification of the number of HARs of the plants in (A). (C) Representative images of 14-day-old Col-0 seedlings grown on 1/2 MS media supplemented with or without 30 μ M 1-NOA in the dark. (D) Quantification of the number of HARs of the plants in (C). The data in (B) and (D) are from three independent biological replicates, with each replicate including 30 seedlings. Data are represented as mean \pm s.e.m. The white scale bars represent 1 cm in (A) and (C).

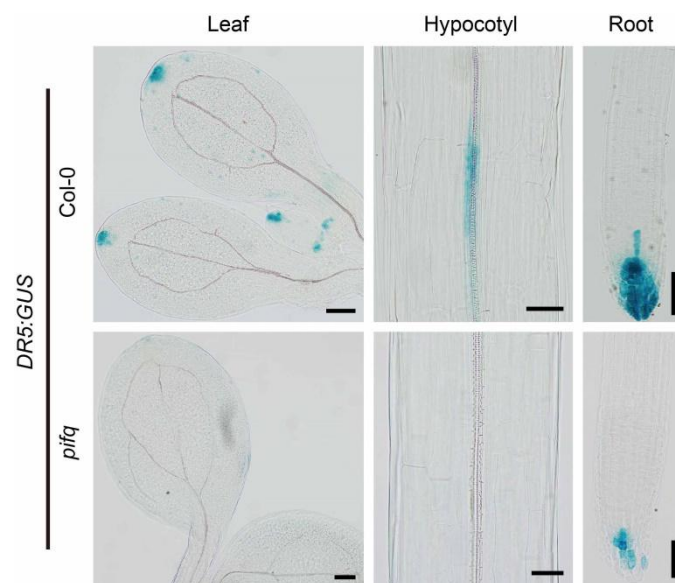


Fig. S5. GUS activity in *DR5:GUS/Col-0* and *DR5:GUS/pifq* plants.

GUS staining of the leaves, roots and hypocotyls of *DR5:GUS/Col-0* and *DR5:GUS/pifq* plants under darkness for 5 days. The black scale bars represent 50 μm .

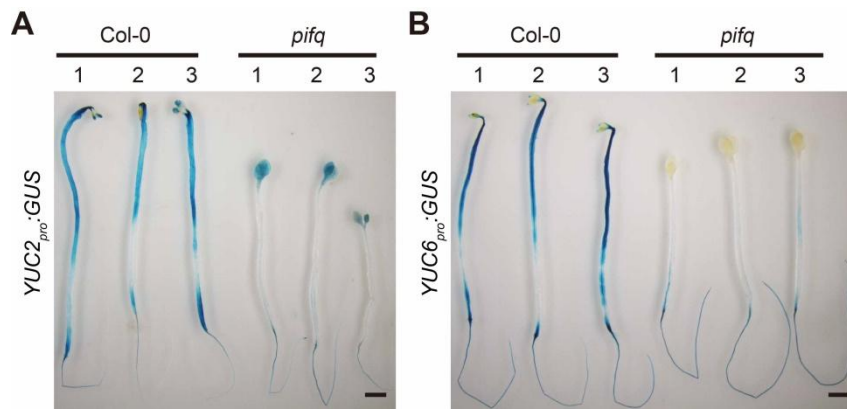


Fig. S6. PIFs promote the expression of *YUC2* and *YUC6*.

(A) GUS staining of the hypocotyls from three independent lines of the *YUC2_{pro}:GUS* transgenic plants in the Col-0 (#1, #2, #3) or *pifq* (#1, #2, #3) mutant background under darkness for 5 days. (B) GUS staining of the hypocotyls from three independent lines of the *YUC6_{pro}:GUS* transgenic plants in the Col-0 (#1, #2, #3) or *pifq* mutant (#1, #2, #3) background under darkness for 5 days. The black scale bars represent 1 mm in (A) and (B).

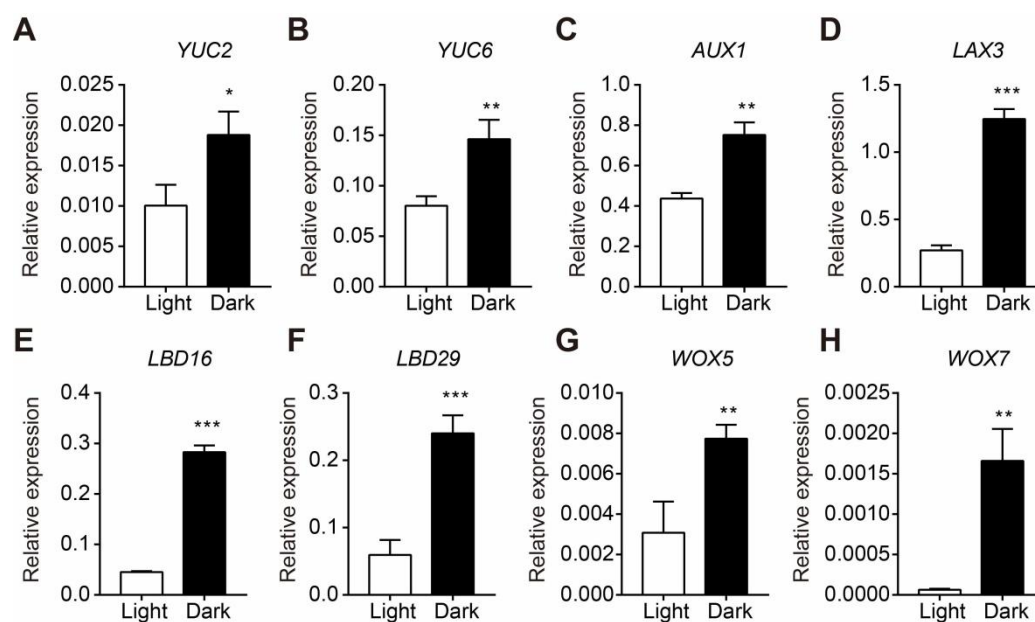


Fig. S7. Expression of the genes related to HAR formation in the hypocotyls of Col-0 under light and darkness.

(A) to (H) qRT-PCR analyses of *YUC2*, *YUC6*, *AUX1*, *LAX3*, *LBD16*, *LBD29*, *WOX5*, and *WOX7* genes expression using the hypocotyls of Col-0 grown in light ($50 \mu\text{mol}\cdot\text{m}^{-2}\cdot\text{sec}^{-1}$) or darkness for 4 days. The averages and SDs were derived from three biological replicates. The asterisks represent significant differences compared with the wild type according to Student's *t* tests (*, $P < 0.05$; **, $P < 0.01$; ***, $P < 0.001$).

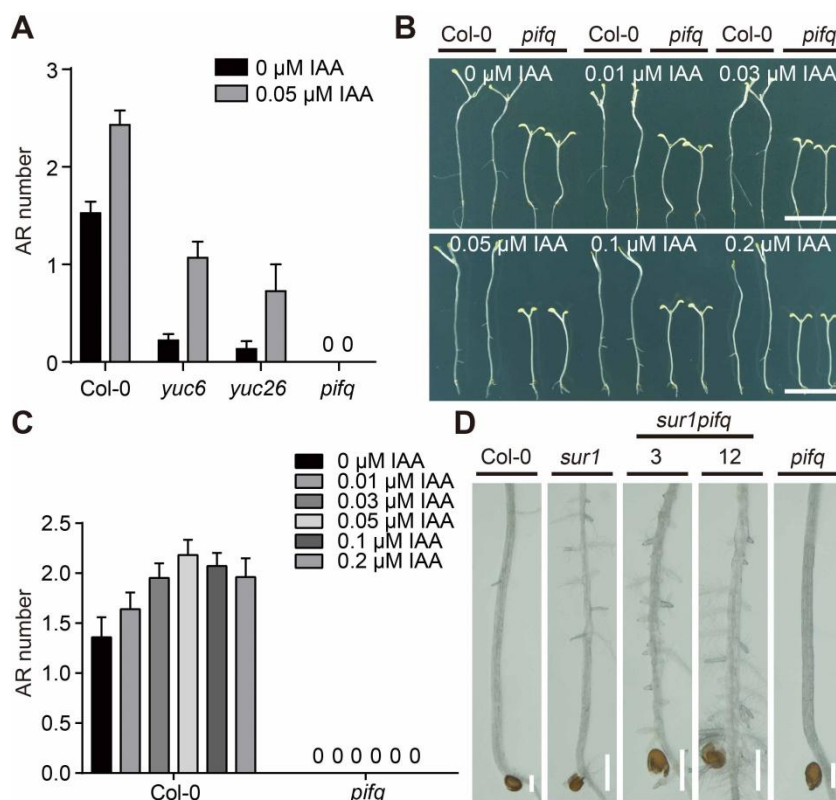


Fig. S8. Endogenous auxin but not exogenous auxin is able to rescue the defective HAR formation of *pifq*.

(A) Quantification of the number of HARs in Col-0, *yuc6* and *yuc26* seedlings grown on 1/2 MS media supplemented with or without 0.05 μM IAA. The data are from three independent biological replicates, with each replicate including 10 seedlings. Data are represented as mean \pm s.e.m. (B) Representative images of 14-day-old Col-0 and *pifq* seedlings grown on 1/2 MS media supplemented with 0, 0.01, 0.03, 0.05, 0.1 or 0.2 μM IAA under darkness. The white scale bars represent 1 cm. (C) Quantification of the number of HARs of the plants in (B). The data in (C) are from three independent biological replicates, with each replicate including 10 seedlings. Data are represented as mean \pm s.e.m. (D) Hypocotyls of 14-day-old Col-0, *sur1* and two independent *sur1 pifq* lines (#3, #12), as viewed through a dissecting microscope. The white scale bars represent 1 mm.

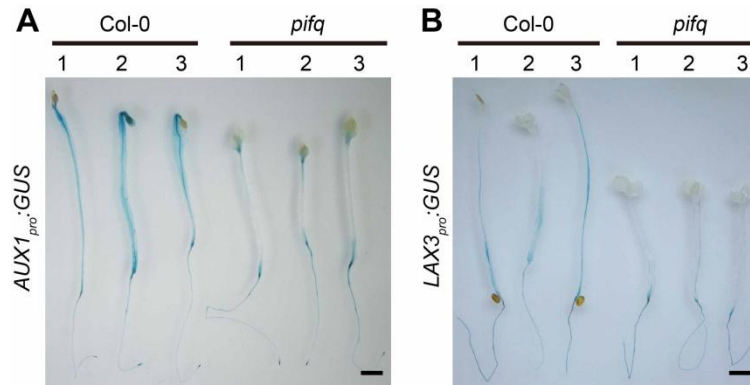


Fig. S9. PIFs promote the expression of *AUX1* and *LAX3*.

(A) GUS staining of the hypocotyls from three independent lines of the *AUX1*_{pro}:*GUS* transgenic plants in the Col-0 (#1, #2, #3) or *pifq* (#1, #2, #3) mutant background under darkness for 5 days. (B) GUS staining of the hypocotyls from three independent lines of the *LAX3*_{pro}:*GUS* transgenic plants in the Col-0 (#1, #2, #3) or *pifq* mutant (#1, #2, #3) background under darkness for 5 days. The black scale bars represent 1 mm in (A) and (B).

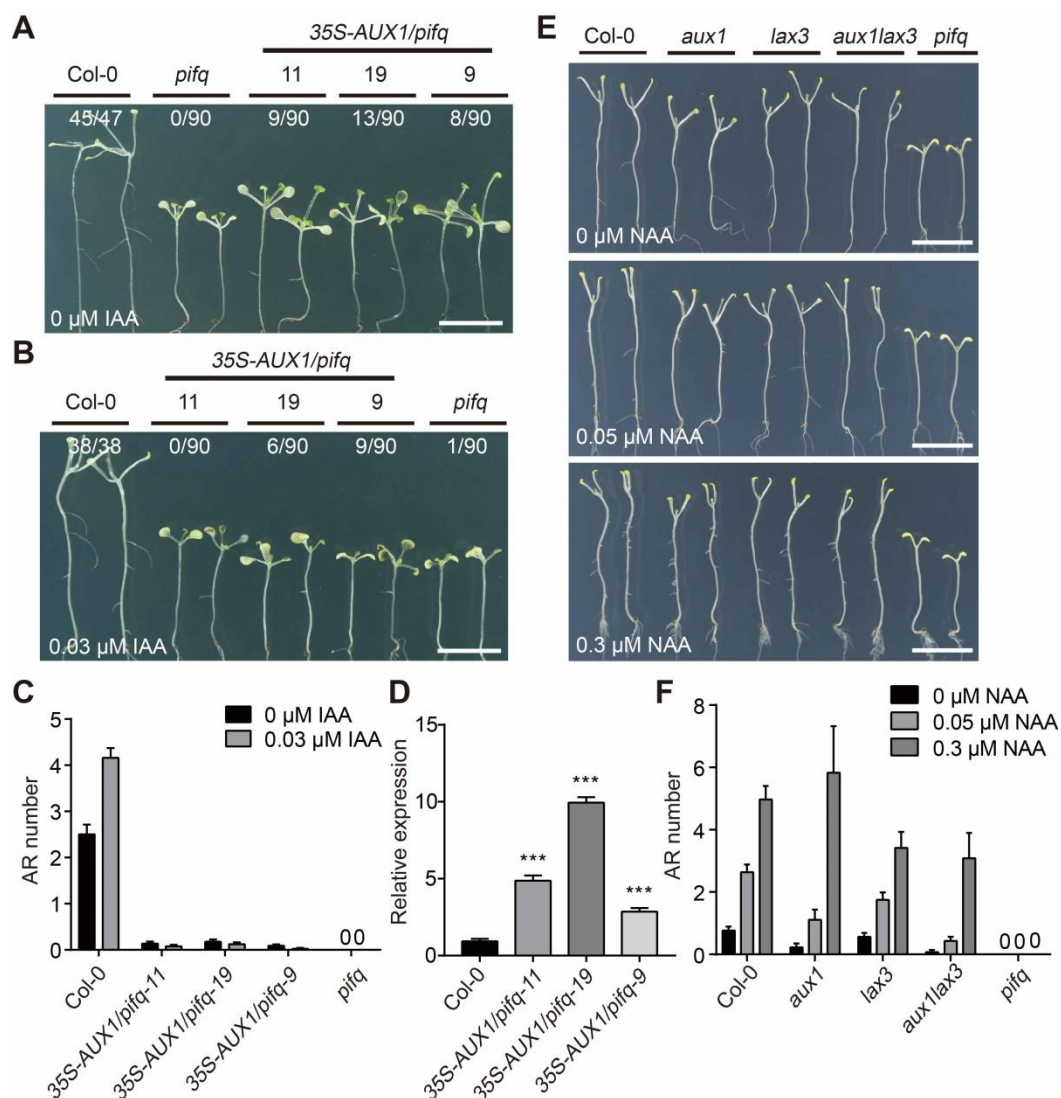


Fig. S10. Overexpression of *AUX1* partially rescues the HAR phenotype of *pifq* in the dark.

(A) and (B) Representative images of 14-day-old Col-0, *35S-AUX1/pifq* (#11, #19, #9) and *pifq* seedlings grown on 1/2 MS media supplemented with or without 0.03 μM IAA. (C) Quantification of the number of HARs of the plants in (A) and (B). The data are from three independent biological replicates, with each replicate including 12 seedlings. Data are represented as mean \pm s.e.m. (D) qRT-PCR results of *AUX1* gene expression in the leaves of 4-week-old Col-0 and *35S-AUX1/pifq* (#11, #19, #9) plants. Data are derived from three biological replicates. Data are represented as mean \pm s.d. The asterisks represent significant differences compared with the wild type according to Student's *t* tests (***, $P < 0.001$). (E) Representative images of 14-day-old Col-0, *aux1*, *lax3*, *aux1 lax3* and *pifq* seedlings grown on 1/2 MS media supplemented with 0, 0.05 and 0.3 μM NAA. (F) Quantification of the number of HARs of the plants in (E). The data are from three independent biological replicates, with each replicate including 10 seedlings. Data are represented as mean \pm s.e.m. The white scale bars represent 1 cm in (A), (B) and (E).

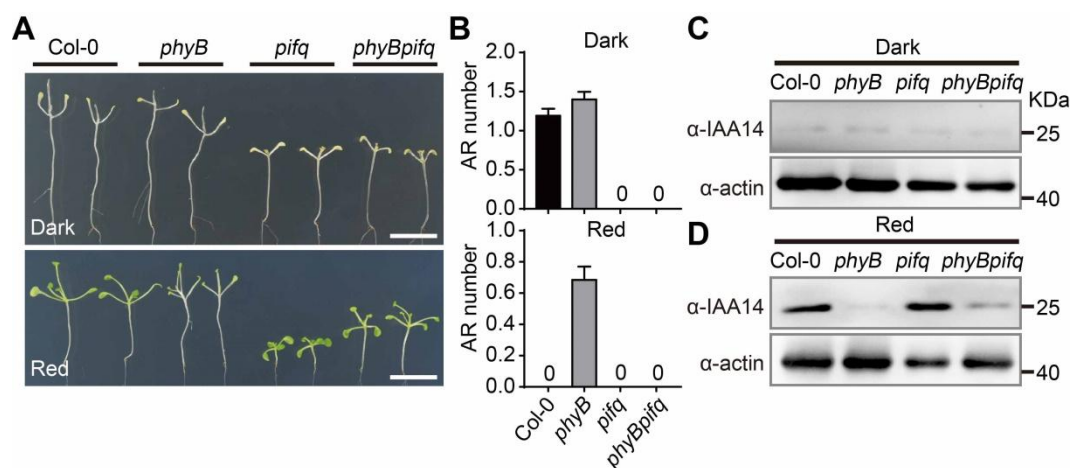


Fig. S11. *PIFs* are epistatic to *PHYB* but do not affect *IAA14* protein levels during HAR formation.

(A) Representative images of 14-day-old Col-0, *phyB*, *pifq* and *phyB pifq* seedlings grown in the dark or red light. The white scale bars represent 1 cm. (B) Quantification of the number of HARs of the plants in (A). The data are from three independent biological replicates, with each replicate including 30 seedlings. Data are represented as mean \pm s.e.m. (C) and (D) Immunoblots showing IAA14 protein levels in 5-day-old Col-0, *phyB*, *pifq* and *phyB pifq* seedlings grown in the dark or red light.

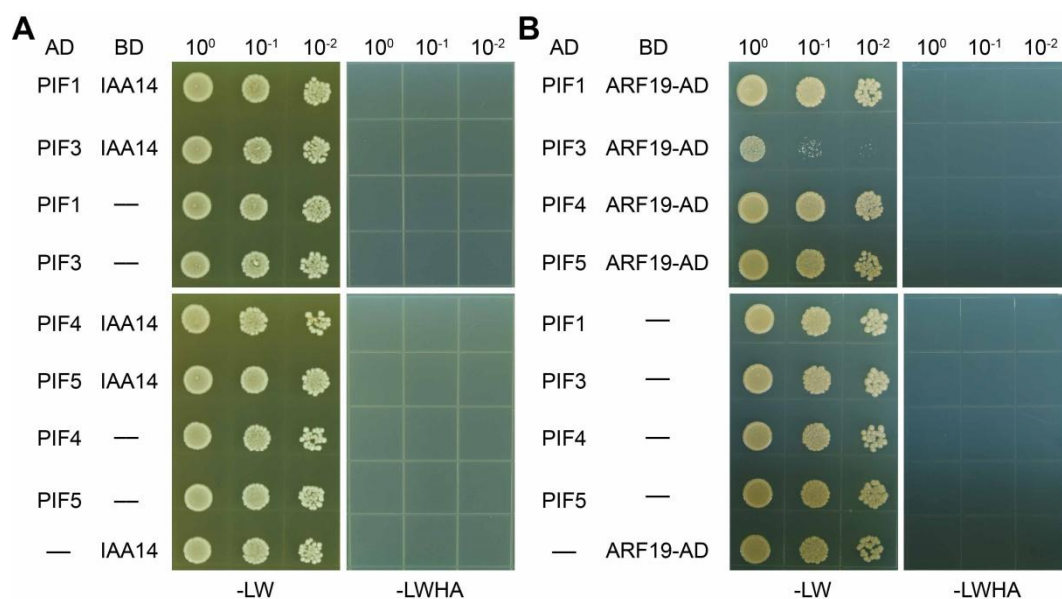


Fig. S12. PIFs do not interact with IAA14 or ARF19.

(A) pGBKT7-IAA14 vectors and pGADT7-PIF1/3/4/5 vectors were cotransformed into yeast cells of the AH109 strain, and empty vectors were transformed as negative controls. The transformed yeast cells were incubated in synthetic media without Leu or Trp (-LW) or in synthetic media without Leu, Trp, His, or adenine (-LWHA). (B) pGBKT7-ARF19-AD (without the activation domain of ARF19) vectors and pGADT7-PIF1/3/4/5 vectors were cotransformed into yeast cells of the AH109 strain, and empty vectors were transformed as negative controls. The transformed yeast cells were incubated in synthetic media without Leu or Trp (-LW) or in synthetic media without Leu, Trp, His, or adenine (-LWHA).

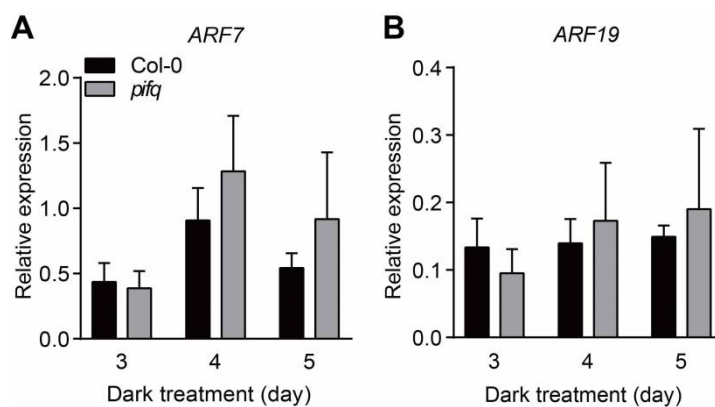


Fig. S13. PIFs do not regulate the expression of *ARF7* or *ARF19*.

(A) and (B) qRT-PCR results of *ARF7* and *ARF19* gene expression in the hypocotyls of Col-0 plants and *pifq* mutants grown in darkness for 3, 4, and 5 days. Data are derived from three biological replicates. Data are represented as mean \pm s.d.

Table S1. List of primers used.

[Click here to download Table S1](#)